Article

Last appearance of *Homo erectus* at Ngandong, Java, 117,000–108,000 years ago

https://doi.org/10.1038/s41586-019-1863-2

Received: 29 May 2019

Accepted: 4 November 2019

Published online: 18 December 2019

Yan Rizal[1,21], Kira E. Westaway[2,21]*, Yahdi Zaim[1], Gerrit D. van den Bergh[3], E. Arthur Bettis III[4], Michael J. Morwood[3,22], O. Frank Huffman[5], Rainer Grün[6], Renaud Joannes-Boyau[7], Richard M. Bailey[8], Sidarto[9], Michael C. Westaway[6,10], Iwan Kurniawan[9], Mark W. Moore[11], Michael Storey[12], Fachroel Aziz[9], Suminto[9,22], Jian-xin Zhao[13], Aswan[1], Maija E. Sipola[14], Roy Larick[15], John-Paul Zonneveld[16], Robert Scott[17], Shelby Putt[18,19] & Russell L. Ciochon[20]*

Homo erectus is the founding early hominin species of Island Southeast Asia, and reached Java (Indonesia) more than 1.5 million years ago[1,2]. Twelve *H. erectus* calvaria (skull caps) and two tibiae (lower leg bones) were discovered from a bone bed located about 20 m above the Solo River at Ngandong (Central Java) between 1931 and 1933[3,4], and are of the youngest, most-advanced form of *H. erectus*[5–8]. Despite the importance of the Ngandong fossils, the relationship between the fossils, terrace fill and ages have been heavily debated[9–14]. Here, to resolve the age of the Ngandong evidence, we use Bayesian modelling of 52 radiometric age estimates to establish—to our knowledge—the first robust chronology at regional, valley and local scales. We used uranium-series dating of speleothems to constrain regional landscape evolution; luminescence, ^{40}argon/^{39}argon (^{40}Ar/^{39}Ar) and uranium-series dating to constrain the sequence of terrace evolution; and applied uranium-series and uranium series–electron-spin resonance (US–ESR) dating to non-human fossils to directly date our re-excavation of Ngandong[5,15]. We show that at least by 500 thousand years ago (ka) the Solo River was diverted into the Kendeng Hills, and that it formed the Solo terrace sequence between 316 and 31 ka and the Ngandong terrace between about 140 and 92 ka. Non-human fossils recovered during the re-excavation of Ngandong date to between 109 and 106 ka (uranium-series minimum)[16] and 134 and 118 ka (US–ESR), with modelled ages of 117 to 108 thousand years (kyr) for the *H. erectus* bone bed, which accumulated during flood conditions[3,17]. These results negate the extreme ages that have been proposed for the site and solidify Ngandong as the last known occurrence of this long-lived species.

Our current understanding of *H. erectus* in Asia largely derives from evidence from the Solo River region of central Java in the Indonesian archipelago[7]. However, this region presents great challenges to constructing solid chronologies for hominin occupation, evolution and dispersal[9]. These problems relate to finding appropriate materials for dating, confusion over the location of previous excavations and find spots, a lack of direct association between the fossils and material being dated, taphonomic differences within the faunal assemblages, reworking of surrounding fluvial deposits and fossils and the leaching of uranium from the fossils being dated. Nowhere are these complications and misperceptions more apparent than at the site of Ngandong[12,18–20].

In 1996, late-Pleistocene age estimates from uranium-series (U-series) and ESR dating were reported for mammalian bone within the 20-m terrace fill at Ngandong and other nearby localities[9]. These unexpectedly young results (corresponding to ages of 53 to 27 kyr) triggered debate regarding the taphonomy of the Ngandong fossil assemblage and the sedimentological context of the dated material[12]. More dating followed: direct gamma-spectrometric ^{230}Th/^{234}U dating of *H. erectus*

[1]Department of Geology, Institute of Technology Bandung, Bandung, Indonesia. [2]Department of Earth and Environmental Sciences, Macquarie University, Sydney, New South Wales, Australia. [3]Centre for Archaeological Science, School of Earth, Atmospheric and Life Sciences, University of Wollongong, Wollongong, New South Wales, Australia. [4]Department of Earth and Environmental Sciences, University of Iowa, Iowa City, IA, USA. [5]Department of Anthropology, University of Texas at Austin, Austin, TX, USA. [6]Australian Research Centre for Human Evolution (ARCHE), Environmental Futures Research Institute, Griffith University, Nathan, Queensland, Australia. [7]Southern Cross GeoScience, Southern Cross University, Lismore, New South Wales, Australia. [8]School of Geography and the Environment, University of Oxford, Oxford, UK. [9]Geology Museum, Geological Agency, Bandung, Indonesia. [10]School of Social Science, University of Queensland, Brisbane, Queensland, Australia. [11]Archaeology and Palaeoanthropology, University of New England, Armidale, New South Wales, Australia. [12]Quadlab, Natural History Museum of Denmark, University of Copenhagen, Copenhagen, Denmark. [13]School of Earth and Environmental Sciences, University of Queensland, Brisbane, Queensland, Australia. [14]Chemistry and Geology Department, Minnesota State University, Mankato, MN, USA. [15]Bluestone Heights, Shore Cultural Center, Cleveland, OH, USA. [16]Department of Earth and Atmospheric Sciences, University of Alberta, Edmonton, Alberta, Canada. [17]Department of Anthropology and Center for Human Evolutionary Studies, Rutgers University, New Brunswick, NJ, USA. [18]The Stone Age Institute, Indiana University, Bloomington, IN, USA. [19]Department of Sociology and Anthropology, Illinois State University, Normal, IL, USA. [20]Department of Anthropology and Museum of Natural History, University of Iowa, Iowa City, IA, USA. [21]These authors contributed equally: Yan Rizal, Kira E. Westaway. [22]Deceased: Michael J. Morwood, Suminto. *e-mail: kira.westaway@mq.edu.au; russell-ciochon@uiowa.edu

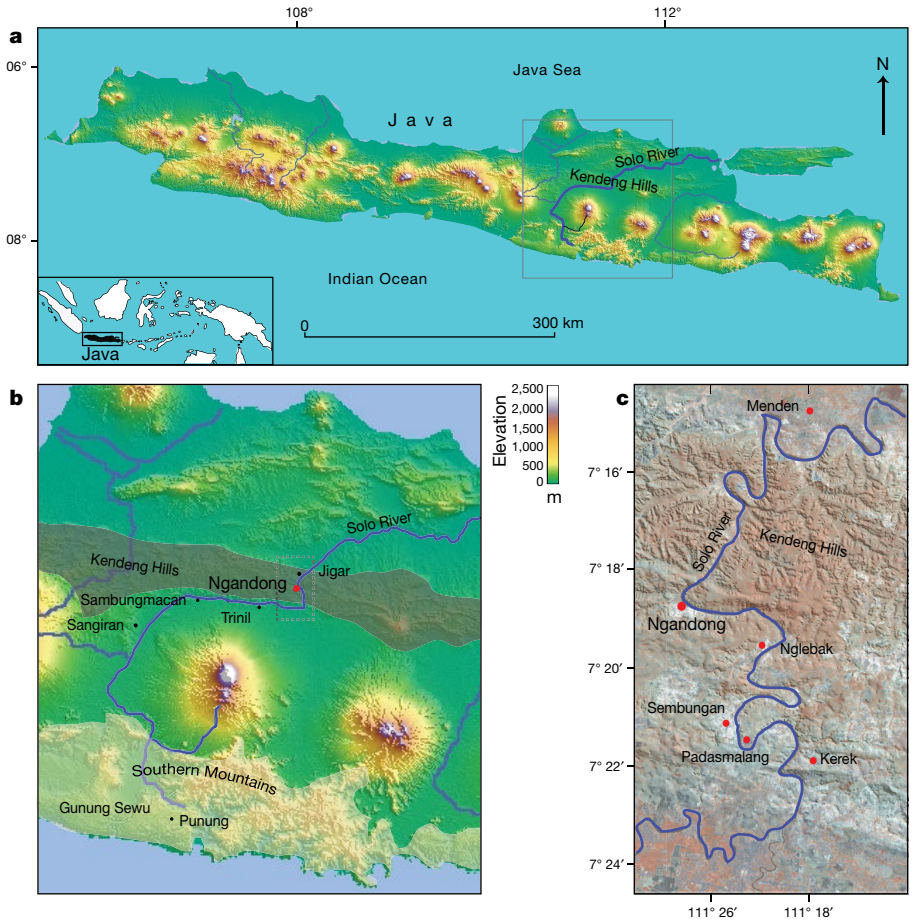

Fig. 1 | Location of Java with *H. erectus* sites and key study sites on the terraces. a, Java and study sites, and the location of Java in the Indonesian archipelago (inset). **b**, The location of the key study areas; the Southern Mountains, Kendeng Hills (Kendeng anticlinorium), Solo River terraces and the *H. erectus* sites of Sangiran, Trinil, Sambungmacan and Ngandong, as well as the other Javanese sites (Jigar and Punung). The scale bar for the elevation changes relates to both **a** and **b**. Topographical map redrawn from the US Geological Survey's Earth Resources Observation and Science Center (USGS EROS). **c**, A section of the Solo River system, from Kerek village in the south to Menden village in the north, showing our key study sites (including Ngandong, Sembungan, Padasmalang, Nglebak, Kerek and Menden). USGS Landsat image with digital elevation model[31,32].

cranial bone from Ngandong and Sambungmacan, giving ages of 40 and 60–70 kyr, respectively[13]; U-series and ESR dating of mammalian bone from Jigar I (downstream of Ngandong), which gave an age of 143 +20 or −17 kyr[14]; and $^{40}Ar/^{39}Ar$ dating of pumice hornblende from Ngandong II and Jigar, giving an age of 546 ± 12 kyr[14] (Fig. 1; uncertainties are defined in figure legends).

To address these chronological inconsistencies, we applied a regional approach to establishing a chronology for the re-excavations that we conducted at Ngandong (Fig. 2). First, to establish a landscape context, we used U-series dating of speleothems to constrain the tectonic uplift of the Southern Mountains that caused the Solo River to divert northward to flow through the Kendeng Hills and form the Solo River strath terrace sequence (Fig. 3, Extended Data Fig. 1). Second, to establish a terrace context, we applied red thermoluminescence, post-infrared infrared-stimulated luminescence (pIR-IRSL) and $^{40}Ar/^{39}Ar$ dating techniques to terrace sediments at localities covering the entire incision sequence: Kerek (upper), Padasmalang (middle), Ngandong (lower), Sembungan terrace (lower, contemporaneous with Ngandong), Ngleback (lowermost) and Menden terrace (outside of the Kendeng Hills and the Solo terrace sequence). We used the terrace chronology to identify the incision phases and constrain the age of the Ngandong terrace by its relative position in the terrace sequence (Extended Data Fig. 2). Third, we established a fossil context by re-excavating the Ngandong bone bed (Extended Data Fig. 6, Supplementary Information section 2) to better understand the sedimentology of the terrace fill, the taphonomy of the Ngandong fossil assemblage and to provide context-supported datable material. We applied laser-ablation U-series analyses[16] to 8 bovid teeth and 15 mammalian long bones (Supplementary Information section 7) and coupled US–ESR analyses to 3 additional fossil bovid teeth (Supplementary Information section 6).

According to the U-series-derived speleothem chronology (Supplementary Table 13), the Gunung Sewu section of the Southern Mountains had been uplifted and the Solo River had been diverted by >500 ka, which places a maximum age on the formation of the terrace sequence. Consistent with this, the red thermoluminescence, pIR-IRSL and $^{40}Ar/^{39}Ar$ chronologies indicate that the sequence of strath terraces was formed between 316 ± 28 and 31 ± 6 ka (with a maximum age of 358 ± 26 kyr), and are all chronologically consistent with their elevation (Extended Data Figs. 2, 8, Supplementary Figs. 1, 2, Supplementary Tables 6, 7, 12).

Our Ngandong excavations yielded a composite cross-section with five lithofacies comprising the Ngandong terrace fill: these lithofacies could be related to terrace-fill descriptions from excavations at the site in the 1930s, which yielded the *H. erectus* calvaria and tibiae[3,15] (Fig. 2, Extended Data Fig. 5, Supplementary Table 1, Supplementary Information section 2). All *H. erectus* fossils recovered in the original excavations were associated with facies C (gravelly sand bars). Our excavations yielded 867 in situ disarticulated non-hominin fossils—mostly isolated teeth and bone fragments, but largely complete elements were also observed[3,17] (Extended Data Fig. 6c, f, g). Usually, these fossils were

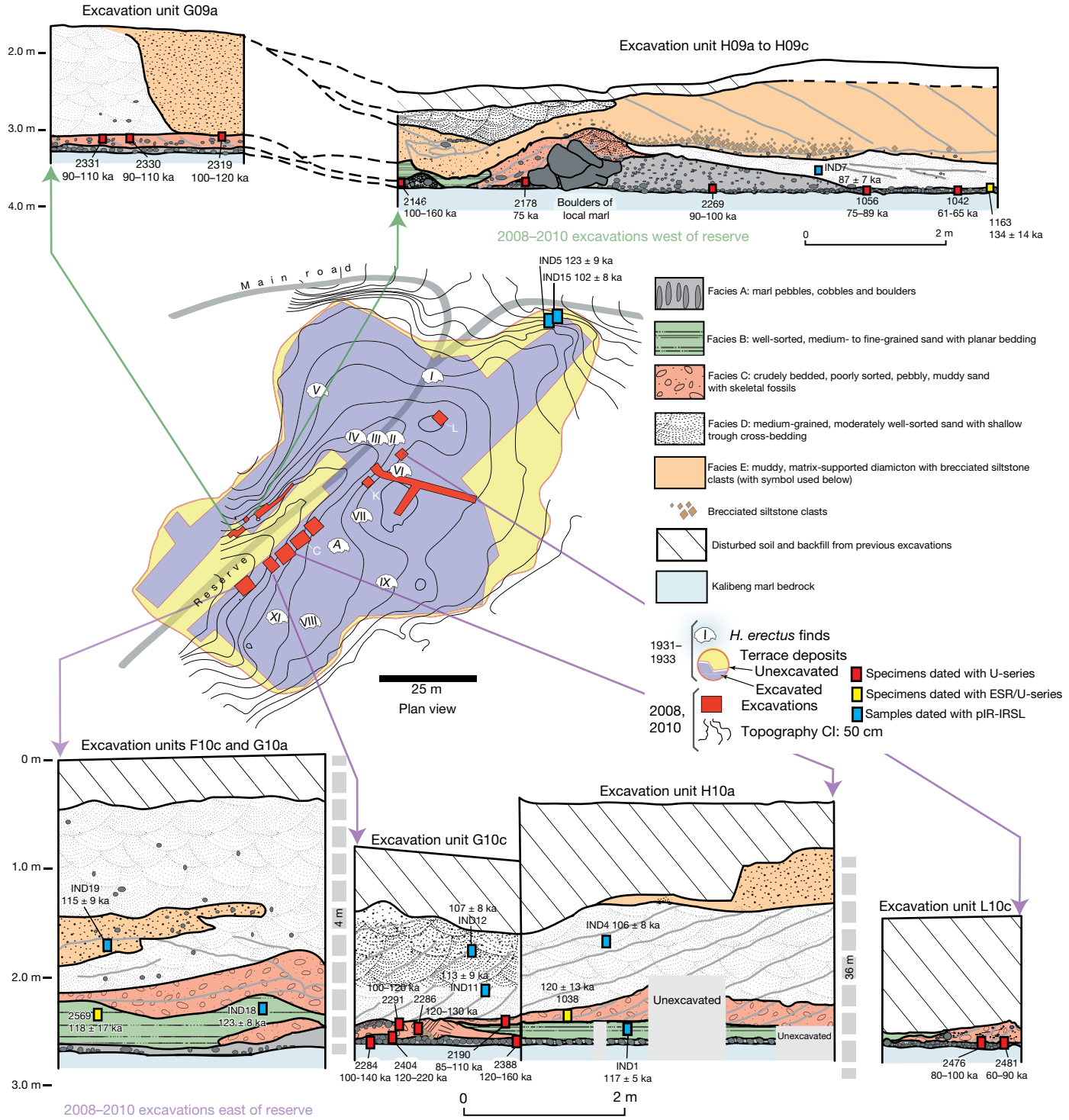

Fig. 2 | Cross-sections of Ngandong site, showing the stratigraphic context and the location of our dating samples. Depositional facies A–E, exposed in excavation bulkheads with collection points for pIR-IRSL samples (IND codes), US–ESR specimens and U-series diffusion–absorption–decay specimens (four-digit specimen numbers) (Supplementary Tables 6, 9, 10). Dated fossils not shown in the figure are 1026 and 1110 from excavation pit C (C on the plan-view map); 1075, 1076 and 1095 from pit L (L); and 1088 from pit K (K). Distances between pits east of the reserve are indicated on the grey dashed columns. The facies are present on the west and east sides of the archaeological reserve, but in different relative abundances. The Ngandong bone bed in facies C was generally excavated away in 1931–1933, but the underlying bone bed in facies A appears to be widely present at the site. The Ngandong *H. erectus* finds are labelled on the plan view map, following a previous publication[3]. I–XI represent the calvaria, and A represents one of the tibiae. Facies A is commonly one or two marl-cobbles thick, but also forms thicker bars. Facies B is moderately well-sorted, fine- to medium-grained sand with shallow-trough and ripple cross-laminations. Facies C is very coarse-grained, very poorly sorted, crudely cross-bedded and partially carbonate-cemented sand and pebbly granule conglomerate. Facies D is moderately well-sorted, medium- to coarse-grained, trough cross-bedded sand. Facies E is sandy gravelly muddy diamicton, which fills channels cut into facies B–D (and into which the bedding inclines). Extended Data Figure 6 and Supplementary Information section 3 provide additional lithological information. Scale bars apply to vertical and horizontal distances. CI, contour interval.

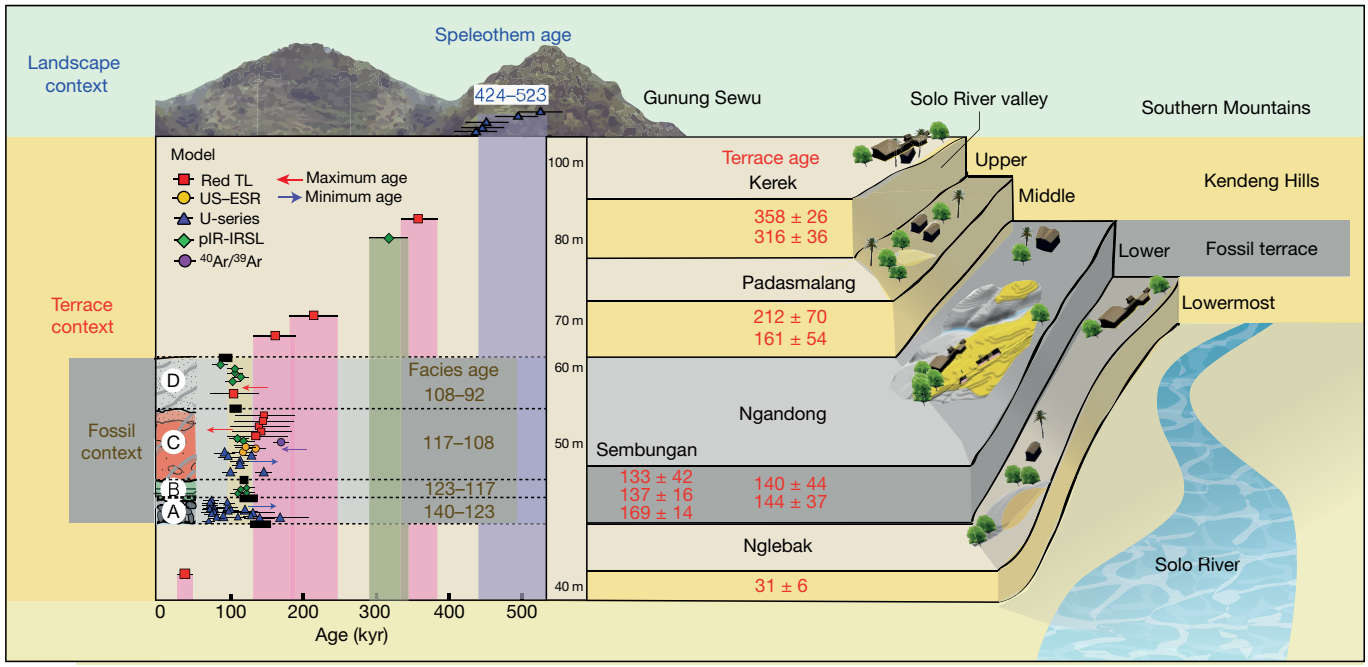

Fig. 3 | A regional chronology for the Ngandong evidence, summarizing the results of our approach. Composite chronology for the landscape, terrace and fossil context for the Ngandong site. All age ranges and errors are presented in kyr. Landscape context: constraining the evolution of the landscape from U-series dating of speleothems ($n = 5$) from the Gunung Sewu region of the Southern Mountains at an altitude of between 340–600 m (mean ages, with s.d. at 2σ uncertainties). Terrace context: from the red thermoluminescence and pIR-IRSL dating of quartz and feldspars, and $^{40}Ar/^{39}Ar$ dating of hornblende from the terrace deposits (mean ages with s.d. at 1σ uncertainties). Five terraces were dated in the region, from the oldest (Kerek; upper) down through Padasmalang (middle), Ngandong (lower), and Sembungan (lower) to Nglebak (lowermost), the youngest ($n = 21$). Relative terrace elevation in metres above mean sea level is shown, but is not to scale. Fossil context: this was provided by the excavations at Ngandong, in which four dating techniques were applied to the fossils and sediments ($n = 26$, mean ages with s.d. at 2σ uncertainties). The composite stratigraphy of the Ngandong terrace is shown. Facies A, B, C and D referring to the same facies shown in Fig. 2, with a thickness of about 2.5 m. All three contexts have been modelled to provide a Bayesian age for the boundaries between the facies at Ngandong (depicted as black rectangles with dashed lines in the model) with the resulting mean age ranges presented at 1σ uncertainties: 140 ± 24 to 123 ± 9 kyr (facies A), 123 ± 9 to 117 ± 6 kyr (facies B), 117 ± 6 to 108 ± 9 kyr (facies C) and 108 ± 9 to 92 ± 16 kyr (facies D). A larger version of this model can be found in Supplementary Information section 11. Symbols correspond to dating techniques: red thermoluminescence, red squares; US–ESR, yellow circles; U-series, blue triangles; pIR-IRSL, green diamonds; $^{40}Ar/^{39}Ar$, purple circle. Red and blue arrows denote maximum and minimum ages, respectively.

encased in a 10–25-cm-thick lens of poorly sorted fossil-rich muddy-pebble conglomerate that was deposited in a sediment-charged river (Fig. 2). Most of the 232 specimens that we analysed were broken before deposition, but more than 90% of them exhibit only minor abrasional rounding (Extended Data Fig. 7). Surface cracking and exfoliation indicative of substantial surface exposure is rare. No fossils show evidence of being reworked from a considerably older formation. Fossils from facies A and facies C have a similar taphonomy but fossils from facies C are larger, and more complete. No stone tools were discovered in this excavation. However, a concentration of 89 artefacts (dated to about 130 ka) was discovered in a contemporaneous Sembungan excavation located upstream of Ngandong (Extended Data Fig. 3, Supplementary Information section 3), and—when combined with the *Elephas* specimen discovered in the older Menden terrace, located downstream of Ngandong (Extended Data Fig. 4, Supplementary Table 5, Supplementary Information section 4)—this evidence provides an occupational context for the Ngandong hominins.

Laser-ablation U-series analysis yielded minimum age estimates of about 120 to 80 kyr and about 140 to 60 kyr for the mammalian long bones and eight bovid teeth, respectively (Extended Data Fig. 9, Supplementary Tables 10, 11). US–ESR dating of three additional bovid teeth provided age estimates corresponding to 134–118 ka (Extended Data Fig. 10, Supplementary Tables 8, 9). These age estimates for the Ngandong fauna agree with the age of deposition of the Ngandong terrace (144 ± 37 to 111 ± 9 kyr), the age of the upper and middle terraces (316 to 161 kyr), the maximum age for the lower terrace at Sembungan (169 ± 14 kyr) and the age of the lowermost terrace (31 ± 6 kyr), according to the red thermoluminescence, pIR-IRSL and $^{40}Ar/^{39}Ar$ dating. When these 52 dating results are entered into a Bayesian model (Fig. 3, Supplementary Tables 14, 15), an age range of 140–92 kyr is established for the deposition of the entire Ngandong terrace sequence, and a range of 117–108 kyr for the bone bed in facies C (Fig. 3), which contained the *H. erectus* material discovered in the 1930s.

Our modelled age range for the Ngandong terrace is substantially older than the direct $^{230}Th/^{234}U$ determinations (40 to 60–70 kyr) that have been reported for the Ngandong *H. erectus* calvaria[13], and is similar to previously reported combined U-series and ESR ages (corresponding to 77 to 143 kyr) for faunal teeth in the terrace at Jigar[14]. However, the upper age limit for the Ngandong site (of about 500 kyr) that was previously suggested on the basis of $^{40}Ar/^{39}Ar$ analyses of water-lain pumice from the Ngandong formation[14], and the age for Ngandong *H. erectus* calvaria of >200 kyr based on gamma-spectrometric U-series techniques[13], are at odds with our proposed age range for the bone bed (117–108 kyr) and our age for the next-oldest terrace in the sequence (162 ± 33 kyr). We believe that our bone-bed chronology is much closer to the actual age of Ngandong *H. erectus*.

Sedimentary and taphonomic observations at Ngandong are best explained by a single flood event, during which facies B, C and D accumulated in rapid succession[17] (Supplementary Information sections 2, 10). A reliable age estimate for the formation of the facies and the non-hominin fossils at Ngandong establishes a depositional age for the *H. erectus* remains (Fig. 2, Supplementary Information sections 5–9). The fossils show only incipient weathering and transport damage, despite being deposited in a river (Extended Data Fig. 7). The

preservation of delicate bony structures[3,17] and soft tissues (Supplementary Table 3) indicate limited exposure. The demise of *H. erectus* and other vertebrates evidently occurred upriver of Ngandong—possibly caused by the changing environmental conditions[17]. The skeletonized and disarticulated remains were then entrained by lahar flows[17] and monsoonal flooding of the Solo River (Supplementary Information section 10). The remains accumulated within large in-channel debris jams[21], owing to the narrowing of the valley at Ngandong, and triggered deposition in channel bars (facies A) and gravelly sand bars (facies C), shortly before sandy bedforms (facies D) and channelized mudflows (facies E) buried the bone beds.

This dated sedimentary and taphonomic framework for the Ngandong bone bed does not support an overlap between modern humans and *H. erectus* in this region[9,18,20]. Instead, the Ngandong fauna in facies A (140 ± 24 ka) pre-dates the rainforest-associated site of Punung (between 128 ± 15 and 118 ± 3 ka)[22], which agrees with the proposed biostratigraphical sequence of Java based on the palaeoenvironmental and associated faunal changes[23]. The *H. erectus* bone bed (facies C) overlaps with Punung and falls within the sea level lowstand at the onset of termination II (around 120 ka)[24]. Thus, it represents the last, dying remnants of the archaic fauna and open woodland environments that were superseded by the impeding rainforest flora and fauna associated with Punung (Supplementary Information section 10).

Furthermore, we can place Ngandong into a regional framework for Island Southeast Asia. *H. erectus* continuously inhabited the island, with dates on Java that start at 1.51 to 0.93 million years ago at Sangiran[1,2], then 540 to 430 ka at Trinil[25] and ending with 117 to 108 ka at Ngandong. *H. erectus* was dispersed widely by 700 ka, as shown by archaeological evidence for hominins at Mata Menge (Flores, Indonesia)[26] and Cagayan Valley (Luzon, Philippines)[27]. Two insular dwarf hominins are found on these outlying islands: *Homo floresiensis* at 100 to 60 ka[28] and *Homo luzonensis* at 66.7 ± 1 ka[29]. Phylogenetic relationships have yet to be determined for these two hominins, but they show morphological similarities with *H. erectus*[29]. Sharing similar temporal ranges, Ngandong *H. erectus*, *H. floresiensis* and *H. luzonensis* represent three evolutionary trajectories of *Homo* in Island Southeast Asia, each of which ended in extinction.

Genomic evidence from modern populations in New Guinea provides estimates for the dates of the arrival of another early hominin in Island Southeast Asia. Two Denisovan lineages diverged from the Altai Denisovans, one at about 363 ka and the other at about 283 ka[30]. These deep divergence dates provide evidence for the early arrival of Denisovans in Island Southeast Asia. Dispersing *Homo sapiens* encountered Denisovan lineages in Island Southeast Asia at about 45.7 ka[30] and at about 29.8 ka[30]. Additionally, a residual signal of approximately 1% archaic DNA in modern regional populations lies outside the human–Neanderthal–Denisovan clade[30]. This may reflect a past introgression event with *H. erectus* and provide evidence that these Denisovans encountered a late-surviving *H. erectus* population.

An increasingly complex picture of hominin evolution in Pleistocene Island Southeast Asia is emerging from fossil and genomic evidence. The chronology of Ngandong *H. erectus* is critical for this narrative. We have approached the age of the Ngandong site in three increasingly precise contexts: the Kendeng Hills landscape, the Solo River terraces and the Ngandong bone bed. Our age estimates for the vertebrate fossils—including *H. erectus*—at Ngandong are, therefore, firmly anchored within their regional chronological and geomorphical contexts. With modelled ages of 117 to 108 kyr, the Ngandong bone bed can finally assume its correct position in the hominin biostratigraphical sequence of Island Southeast Asia.

Online content

Any methods, additional references, Nature Research reporting summaries, source data, extended data, supplementary information, acknowledgements, peer review information; details of author contributions and competing interests; and statements of data and code availability are available at https://doi.org/10.1038/s41586-019-1863-2.

1. Larick, R. et al. Early Pleistocene $^{40}Ar/^{39}Ar$ ages for Bapang Formation hominins, Central Jawa, Indonesia. *Proc. Natl Acad. Sci. USA* **98**, 4866–4871 (2001).
2. Zaim, Y. et al. New 1.5 million-year-old *Homo erectus* maxilla from Sangiran (Central Java, Indonesia). *J. Hum. Evol.* **61**, 363–376 (2011).
3. Huffman, O. F., de Vos, J., Berkhout, A. W. & Aziz, F. Provenience reassessment of the 1931–1933 Ngandong *Homo erectus* (Java), confirmation of the bonebed origin reported by the discoverers. *Paleoanthropology* **2010**, 1–60 (2010).
4. Oppenoorth, W.F.F. Een nieuwe fossiele mensch van Java. *Tijdschrift van het Koninklijk Nederlandsch Aardrijkskundig Genootschap* **XLIX**, 704–708 (1932).
5. Frankel, M. Notes from an excavation. *Nature* https://doi.org/10.1038/news.2010.377 (2010).
6. Santa Luca, A. P. *The Ngandong Fossil Hominids: A Comparative Study of a Far Eastern* Homo erectus *Group* Yale University Publications in Anthropology 78 (Yale Peabody Museum, 1980).
7. Rightmire, G. P. *The Evolution of* Homo erectus: *Comparative Anatomical Studies of an Extinct Human Species* (Cambridge Univ. Press, 1990).
8. Schwartz, J. H. & Tattersall, I. *The Human Fossil Record: Volume Four – Craniodental Morphology of Early Hominids (Genera* Australopithecus, Paranthropus, Orrorin*) and Overview* (Wiley, 2005).
9. Swisher, C. C. III et al. Latest *Homo erectus* of Java: potential contemporaneity with *Homo sapiens* in southeast Asia. *Science* **274**, 1870–1874 (1996).
10. Bartstra, G.-J. et al. Ngandong man: age and artifacts. *J. Hum. Evol.* **17**, 325–337 (1988).
11. Rizal, Y. *Die Terrasse Entlang des Solo-Flusses in Mittel und Ost-Java, Indonesien.* PhD thesis, Universität zu Köln (1998).
12. Grün, R. & Thorne, A. Dating the Ngandong humans. *Science* **276**, 1575–1576 (1997).
13. Yokoyama, Y., Falguères, C., Sémah, F., Jacob, T. & Grün, R. Gamma-ray spectrometric dating of late *Homo erectus* skulls from Ngandong and Sambungmacan, Central Java, Indonesia. *J. Hum. Evol.* **55**, 274–277 (2008).
14. Indriati, E. et al. The age of the 20 meter Solo River terrace, Java, Indonesia and the survival of *Homo erectus* in Asia. *PLoS ONE* **6**, e21562 (2011).
15. Ciochon, R. L. et al. Rediscovery of the *Homo erectus* bed at Ngandong: site formation of a late Pleistocene hominin site in Asia. *Am. J. Phys. Anthropol.* **48**, 106 (2009).
16. Sambridge, M., Grün, R. & Eggins, S. U-series dating of bone in an open system: the diffusion-absorption-decay model. *Quat. Geochronol.* **9**, 42–53 (2012).
17. Huffman, O. F. et al. Mass death and lahars in the taphonomy of the Ngandong *Homo erectus* bonebed, and volcanism in the hominin record of eastern Java. *Paleoanthropology* **2010**, abstr. A14 (2010).
18. Westaway, M. C. Preliminary observations on the taphonomic processes at Ngandong and some implications for a late *Homo erectus* survivor model. *Tempus* **7**, 189–193 (2002).
19. Westaway, M., Jacob, T., Aziz, F., Otsuka, H. & Baba, H. Faunal taphonomy and biostratigraphy at Ngandong, Java, Indonesia and its implications for the late survival of *Homo erectus*. *Am. J. Phys. Anthropol.* **120**, abstr. 222–223 (2003).
20. Westaway, M. C. & Groves, C. P. The mark of ancient Java is on none of them. *Archaeol. Ocean.* **44**, 84–95 (2009).
21. Jenkins, K. et al. New excavations of a Late Pleistocene bonebed and associated MSA artifacts from Rusinga Island, Kenya. *Paleoanthropology* **2012**, abstr. A17 (2012).
22. Westaway, K. E. et al. Age and biostratigraphic significance of the Punung rainforest fauna, East Java, Indonesia, and implications for *Pongo* and *Homo*. *J. Hum. Evol.* **53**, 709–717 (2007).
23. de Vos, J. The *Pongo* faunas from Java and Sumatra and their significance for biostratigraphical and paleo-ecological interpretations. *Proc. Koninklijke Nederlandse Akademie van Wetenschappen, Series B* **86**, 417–425 (1983).
24. Railsback, L. B., Gibbard, P. L., Head, M. J., Voarintsoa, N. R. G. & Toucanne, S. An optimized scheme of lettered marine isotope substages for the last 1.0 million years, and the climatological nature of isotope stages and substages. *Quat. Sci. Rev.* **111**, 94–106 (2015).
25. Joordens, J. C. et al. *Homo erectus* at Trinil on Java used shells for tool production and engraving. *Nature* **518**, 228–231 (2015).
26. Brumm, A. et al. Age and context of the oldest known hominin fossils from Flores. *Nature* **534**, 249–253 (2016).
27. Ingicco, T. et al. Earliest known hominin activity in the Philippines by 709 thousand years ago. *Nature* **557**, 233–237 (2018).
28. Sutikna, T. et al. Revised stratigraphy and chronology for *Homo floresiensis* at Liang Bua in Indonesia. *Nature* **532**, 366–369 (2016).
29. Détroit, F. et al. A new species of *Homo* from the Late Pleistocene of the Philippines. *Nature* **568**, 181–186 (2019).
30. Jacobs, G. S. et al. Multiple deeply divergent Denisovan ancestries in Papuans. *Cell* **177**, 1010–1021 (2019).
31. Suminto, M. M., Sidarto, Maryanto, S., Susanto, E. E., Aziz, S. F., Christiana, I., & Fitriani, E. *A Study of the Solo River Terraces from Kerek to Karsono: Ngawi and Bojonegoro Regions, East Java* (Geological Research and Development Centre, 2004).
32. Sidarto & Morwood, M. J. Solo River terrace mapping in the Kendeng Hills area, Java: use of landsat imagery and digital elevation model overlays. *J. Sumber Daya Geologi* **14**, 196–207 (2004).

Methods

To constrain age range of the Ngandong fossils, we considered three interrelated components: a landscape context, a terrace context and a fossil context.

Establishing the landscape context

The landscape evolution of central Java followed this sequence of events: (1) the seismic uplift of the Southern Mountains, (2) the northward diversion of the Solo River through the Kendeng Hills and (3) the resulting terrace formation, including that of the Ngandong terrace[33,34]. The timing of these events can be constrained by establishing the age of the oldest speleothem deposits in the Gunung Sewu (Fig. 1b) using U-series dating, which provides a minimum age for the uplift of the Southern Mountains, the diversion of the Solo River and the subsequent uplift of the Kendeng anticlinorium (which created the Kendeng Hills)—and thus a maximum age for terrace formation in the Solo River valley.

U-series dating of speleothems. U-series dating of flowstones and stalagmites provides minimum ages for the karstification of the Gunung Sewu, which was initiated by the uplift of the Southern Mountains. Calcite was sampled from the outer edges of the stalagmites using a hammer and chisel. Calcite crystals that were free of any weathered surfaces were extracted from each of these samples, and cleaned ultrasonically to remove as much sediment contamination as possible before they were subjected to chemical treatment and isotopic measurements by mass spectrometry[35]. U-series dating of the speleothem samples was conducted in the Radiogenic Isotope Facility (The University of Queensland), using a VG Sector 54 thermal ionization mass spectrometer (TIMS) and a Nu Plasma multi-collector inductively coupled mass spectrometer (MC-ICP-MS). Analytical procedures followed previous publications for TIMS and MC-ICP-MS[35–37]. $^{230}Th/^{234}U$ ages were calculated using Isoplot EX 3.75 (ref. [38]), and half-lives of 75,690 years (^{230}Th) and 245,250 years (^{234}U)[39].

Establishing the terrace context

As strath river terraces form in a sequence (with the oldest at the highest elevation and the youngest at the lowest), the age of the oldest Solo River terraces at Kerek (upper) and the youngest in Nglebak (lowermost) provide a maximum and minimum age range for the Ngandong terrace.

Strategy for identifying and dating the terraces. Initial mapping work in this region involved the use of digital elevation maps of the terraces created from a Landsat image (ETM7+ using bands 4, 5 and 7 merged with band 8) overlying a 1:25,000 topographical map, to produce a 15-m resolution digital elevation model[31,32]. Suitable sites were then chosen from each of the four identified terraces (lowermost, lower, middle and upper) within a designated study section from Kerek village in the south to Sunggun village in the north (Fig. 1c, Extended Data Fig. 1f). Compared to Sangiran and Mojokerto, the site of Ngandong is within much-younger clastic terrace deposits, which presents an opportunity to constrain the age of the deposition of the terrace using luminescence dating. This technique has yet to be successfully applied to this river system. The nature of the quartz and feldspar grains in this volcanic province is challenging, with no usable blue signal and high anomalous fading, respectively. This necessitates the use of red thermoluminescence dating techniques on quartz grains[40,41] and pIR-IRSL on feldspars[42]. This is supported by $^{40}Ar/^{39}Ar$ techniques on in situ pumice lens in the alluvium at Sembungan (low terrace).

Luminescence dating of quartz and feldspar grains from the fluvial terraces. At each site, a suitable sampling location was chosen, a section was dug to expose the terrace sediments and the stratigraphic characteristics were recorded. Sampling for luminescence dating was conducted using either opaque PVC pipes banged into the terrace (laboratory codes IND1–18 and NGD1–3) or—for the more-cemented terrace sediments—bulk sampling was conducted at night using subdued red-light conditions (laboratory code KER1). Quartz and feldspars grains of 90–125 μm were separated using standard purification procedures, including a final etch in 40% hydrofluoric acid for 45 min and 10% for 10 min, respectively, to remove the external alpha-dosed rinds[43]. The Solo River terraces yielded small amounts of quartz: 60 mg, with about 20 mg used for aliquots A and B of the dual-aliquot protocol (DAP) procedure[44] to derive the D_e estimates (Supplementary Table 6), and only about 40 mg remaining for additional testing. Therefore, feldspars were also analysed to support the sedimentary chronology, which also yielded small—but usable—amounts. All luminescence analysis was conducted at the 'Traps' luminescence dating facility at Macquarie University.

Using a DAP[44], isothermal red thermoluminescence emissions from quartz were detected using a red-sensitive photomultiplier tube (Electron Tubes S20 9658B). Quartz grains were mounted on stainless-steel discs using silicone oil spray; each large aliquot was composed of about 5,000 grains (around 10 mg). The isothermal red thermoluminescence emissions[45–47] were measured using a red-sensitive photomultiplier tube (Electron Tubes 9658B) and cooling tower (LCT50 liquid-cooled thermoelectric housing) with Kopp 2-63 and BG-39 filter combination[45]. Laboratory irradiations were conducted using a calibrated $^{90}Sr/^{90}Y$ beta source. D_e values were estimated from the 20–30-s interval of isothermal decay (which was bleachable by >380-nm illumination) using the final 160 s as background. Aliquots were heated to 260 °C at a heating rate of 5 K s^{-1} and then held at 260 °C for 1,000 s to minimize the unwanted thermoluminescence from incandescence.

To overcome the problems of anomalous fading[48], we adopted a standard pIR-IRSL protocol for single aliquots of feldspars using a 300 °C preheat and 270 °C pIR-IRSL stimulation combination, following a standard 50-°C infrared stimulation. The use of single-grain feldspar techniques was investigated but low sample sensitivities yielded very low acceptance rates (<0.5%) that were not practical considering the small amounts of sample yield. pIR-IRSL measurements were thus conducted on single aliquots of feldspars using infrared (875-nm) light-emitting diodes at 80% power for 200 s (to enable a long stimulation), and the emissions were detected using Schott BG-39 and Corning 7-59 filters to transmit wavelengths of 320–480 nm (ref. [49]). Four procedural tests were applied to small aliquots of about 1,000 grains using the following preheat and infrared stimulation combinations: (1) 250 and 225 °C (refs. [48,50]), (2) 280 and 250 °C (ref. [51]), (3) 300 and 270 °C (ref. [51]) and (4) 320 and 290 °C (refs. [52,53]). The tests were: (1) a preheat plateau test using 3 discs; (2) fading tests, including a prompt, 1-h, 10-h and 1-week delay; (3) bleaching tests using 1 fresh aliquot per temperature to determine the amount of residual IRSL after an extended bleach of 4 h in a solar simulator; and (4) dose recovery tests using 8 bleached aliquots (bleached using a solar simulator for 4 h) and a surrogate dose of 200 Gy. From these tests, it was determined that the 270-°C stimulation and 300-°C preheat combination plotted within the flattest part of the preheat plateau, provided the best recovery of the surrogate dose, with the least fading of all of the pIR-IRSL signals (g value = between 1.6–2.2% per decade) and lowest residual value (<10 Gy). In total, 24 aliquots were used to conduct a modified single-aliquot regenerative-dose (SAR) procedure. These resulting age estimates were corrected according to the results of the anomalous fading tests (using a weighted mean fading rate of 1.9 ± 0.3% per decade), but no residual corrections were undertaken.

Measurements of ^{238}U, ^{235}U, ^{232}Th (and their decay products) and ^{40}K were estimated using Geiger–Muller multi-counter beta-counting of dried and powdered sediment samples in the laboratory, and a portable gamma spectrometer in the field. The corresponding (dry) beta and gamma dose rates were obtained using previously published conversion factors[54] and beta-dose attenuation factors[55]. An effective internal

alpha dose rate of 0.03 Gy kyr^{-1} (ref. [56]) and 0.72 Gy kyr^{-1} (refs. [57,58]) were used for the 90–125-μm quartz and feldspar samples, respectively (owing to the radioactive decay of ^{40}K and ^{87}Rb), which were made assuming K (12.5 ± 0.5%)[57] and ^{87}Rb (400 ± 100 μg g^{-1})[58] concentrations, and was included in the total dose rate. Cosmic-ray dose rates were estimated from published relationships[59], making allowance for the sediment overburden at the sample locality (about 0.5-4.0 m), the altitude (around 60 m above sea level) and geomagnetic latitude and longitude (7° and 111°) of the sampling site. The total dose rate was calculated using a long-term water content of 5–15 ± 2%, which is close to the measured (field) water content of 5–15%. High-resolution gamma spectrometry of the powdered sediment samples was also conducted to test for disequilibrium within the uranium decay chain (Supplementary Table 7).

^{40}Ar/^{39}Ar dating of a pumice lens in the Sembungan terrace. ^{40}Ar/^{39}Ar dating of single and multiple hornblende crystals was conducted on a pumice lens (sample SS59B) taken from the middle of the Sembungan terrace, to provide the eruption age of the pumice and a maximum age of deposition for the terrace. The 10-cm-thick pumice lens was exposed in the western quarry wall over a length of 2.2 m at a depth of 2.0 m below datum, and 2.1 m above the base of the terrace fill. Euhedral hornblende crystals up to 1 mm in length were hand-picked under a binocular microscope and loaded into wells in aluminium sample discs (diameter 18 mm) for neutron irradiation, along with the astronomically calibrated 1.185-million-year-old Alder Creek sanidine[60] as the neutron fluence monitor. Neutron irradiation was performed for 0.25 h in the cadmium-shielded CLICIT facility at the Oregon State University TRIGA reactor.

Argon isotopic analyses of the gas released by laser fusion of hornblende crystals (Supplementary Table 12) was done on a fully automated, Nu Instruments Noblesse multi-collector noble-gas mass spectrometer, using previously documented instrumentation and procedures[61,62].

Estimating downcutting rates. We used the terrace chronology to establish downcutting rates for the Solo Valley in the Kendeng Hills. These rates were established by dividing the age of each alluvial terrace (in thousands of years) (Supplementary Table 6), by the distance of downcutting between each terrace (mm) to provide a downcutting rate (in millimetres per thousand years (mm kyr^{-1})) for each terrace level. Then, the age of the highest terrace was divided by the total distance to the river (66 m) to estimate an overall rate of downcutting (in mm kyr^{-1}) for the entire valley (Supplementary Information section 15). The mean errors associated with these red thermoluminescence and pIR-IRSL ages have been propagated through to the final downcutting rate, to obtain an error margin of ±8%.

Establishing the fossil context

The strategy for the Ngandong excavation consisted of locating the backfilled edges of the original excavated area along the margins of the original Netherlands Indies Survey reserve, using maps produced during the 1931–1933 excavations[3]. Our 115-m^2 excavation footprint encompassed several pits that paralleled the edges of the excavation reserve. We identified five lithofacies, comprising the terrace fill at Ngandong, and developed a composite cross-section that illustrated lateral facies relationships and the context of the bone bed within the sequence of deposits (Fig. 2, Supplementary Table 2). Attempts to date fossil teeth from facies A and facies C using radiocarbon were unsuccessful, as was initial optically stimulated luminescence dating of quartz from sediments. However, red thermoluminescence and pIR-IRSL dating of quartz and feldspars, respectively, from overbank terrace deposits, and U-series dating of fossil teeth and bones proved effective.

Laser-ablation U-series dating of fossil bone and teeth. Fifteen bone samples for U-series dating were collected during the 2010 field season (sample numbers 2146, 2178, 2190, 2216, 2269, 2284, 2286, 2291, 2319, 2330, 2331, 2388, 2404, 2476 and 2481) from facies A and facies C. Figure 2 gives the relative positions of these samples. Laser-ablation mass spectrometry to measure U-series isotopes along the cross-sections of these dense, mammalian long-bone fossils was carried out at the Australian National University[39,63–66] (Extended Data Fig. 9). Uranium and thorium concentrations were derived from repeated measurements of the NBS-610 standard, uranium-isotope ratios from the dentine of a rhinoceros tooth from Hexian[67]. Spot analyses were used, which have the advantages over continuous tracks by being able to avoid pores and optimize measurement conditions as well as counting statistics for each analysis. The laser was kept in one position for 100 s, ablating a small pit (132 μm in diameter, approximately 50 to 100-μm deep) in the bone. To address U-series age issues related to uncertainties in open-system uranium uptake, the ^{230}Th/^{238}U and ^{234}U/^{238}U datasets for each bone were fitted using a diffusion–absorption–decay model[68].

Coupled US–ESR dating of fossil teeth. Bovid molars were collected for US–ESR direct dating, and sectioned using a large diamond-blade rotating saw and polished to a 100-μm surface smoothness. Samples NDG-1038, NDG-1163, NDG-2074, NDG-2562, NDG-2566 and NDG-2569 were first analysed by laser-ablation ICP-MS (LA-ICPMS) quadrupole for uranium distribution, to assess the suitability of the samples for US–ESR dating. Only the samples NDG-1038, NDG-1163 and NDG-2569 were found to be suitable, and these samples were prepared following a previously developed protocol[66] (Extended Data Fig. 10). Each fragment was then measured at Southern Cross University on a Freiberg MS5000 ESR X-band spectrometer, and irradiated with the Freiberg X-ray irradiation chamber. ESR intensities were extracted from the merged spectra obtained from angular variation measurements[69,70] (for an example, see Extended Data Fig. 10b), after correcting for baseline, subtraction of isotropic signals and assessment of the contribution of non-oriented CO_2^- radicals (NOCORs) using previously published protocols[66,70] (for an example, see Extended Data Fig. 10c). Dose–response curves were obtained using the MCDOSE 2.0 software[71] (Extended Data Fig. 10a). U-series dating was conducted on both dentine and enamel at the University of Wollongong, using an ESI NW193 ArF Excimer laser coupled to a MC-ICP-MS Neptune Plus to calculate the internal dose rate. All age calculations were carried out with the US–ESR program[72], which uses previously published[73] dose rate conversion factors.

Modelling of landscape, terrace and excavation chronologies

To evaluate the uncertainties of the integrated dating approach of the landscape, terrace and fossil contexts (Supplementary Tables 6, 9, 10, 12, 13), Bayesian modelling was performed on all independent age estimates using the OxCal (version 4.2) software[74] available at https://c14.arch.ox.ac.uk/oxcal.html (Supplementary Tables 14, 15). The analysis incorporated the probability distributions of individual ages, and constraints imposed by stratigraphic relationships and the reported minimum or maximum nature of some of the individual age estimates. Each individual age was included as a Gaussian distribution (with mean and s.d. defined by the age estimate and their associated uncertainties). The U-series profiling ages on the fossil bone yielded a range of ages (160–60 kyr) and these were incorporated as a uniform distribution over this interval.

Data reporting

No statistical methods were used to predetermine sample size. The experiments were not randomized and investigators were not blinded to allocation during experiments and outcome assessment.

Reporting summary

Further information on research design is available in the Nature Research Reporting Summary linked to this paper.

Data availability

The data that support the findings of this study are included in the Supplementary Information. Additional data are available from the corresponding authors upon reasonable request.

Code availability

The Oxcal code used for the Bayesian model in this study is included in Supplementary Table 15.

33. Simandjuntak, T. O. & Barber, A. J. in *Tectonic Evolution of Southeast Asia (Geological Society Special Publication No. 106)* (eds Hall, R. & Blundell, D. J.) 185–201 (Geological Society of London, 1996).
34. Berghuis, H. W. K. & Troelstra, S. R. Plio-Pleistocene foraminiferal biostratigraphy of the eastern Kendeng zone (Java, Indonesia): the Marmoyo and Sumberingin sections. *Palaeogeogr. Palaeoclimatol. Palaeoecol.* **528**, 218–231 (2019).
35. Zhou, H. Y., Zhao, J. X., Wang, Q., Feng, Y. X. & Tang, J. Speleothem-derived Asian summer monsoon variations in central China during 54–46 ka. *J. Quat. Sci.* **26**, 781–790 (2011).
36. Clark, T. R. et al. Discerning the timing and cause of historical mortality events in modern *Porites* from the Great Barrier Reef. *Geochim. Cosmochim. Acta* **138**, 57–80 (2014).
37. Ludwig, K. R. *User's Manual for Isoplot 3.75. A Geochronological Toolkit for Microsoft Excel (Berkeley Geochronology Center Special Publication No. 5)* (Berkeley Geochronological Center, 2012).
38. Cheng, H. et al. The half-lives of uranium-234 and thorium-230. *Chem. Geol.* **169**, 17–33 (2000).
39. Eggins, S. M. et al. In situ U-series dating by laser-ablation multi-collector ICPMS: new prospects for Quaternary geochronology. *Quat. Sci. Rev.* **24**, 2523–2538 (2005).
40. Morwood, M. J. et al. Archaeology and age of a new hominin from Flores in eastern Indonesia. *Nature* **431**, 1087–1091 (2004).
41. Morwood, M. J. et al. Further evidence for small-bodied hominins from the Late Pleistocene of Flores, Indonesia. *Nature* **437**, 1012–1017 (2005).
42. Westaway, K. E. et al. An early modern human presence in Sumatra 73,000–63,000 years ago. *Nature* **548**, 322–325 (2017).
43. Huntley, D. J., Godfrey-Smith, D. I. & Thewalt, M. L. W. Optical dating of sediments. *Nature* **313**, 105–107 (1985).
44. Westaway, K. E. & Roberts, R. G. A dual-aliquot regenerative-dose protocol (DAP) for thermoluminescence (TL) dating of quartz sediments using the light-sensitive and isothermally stimulated red emissions. *Quat. Sci. Rev.* **25**, 2513–2528 (2006).
45. Spooner, N. A. & Franklin, A. D. Effect of the heating rate on the red TL of quartz. *Radiat. Meas.* **35**, 59–66 (2002).
46. Murray, A. S. & Mejdahl, V. Comparison of regenerative-dose single-aliquot and multiple-aliquot (SARA) protocols using heated quartz from archaeological sites. *Quat. Sci. Rev.* **18**, 223–229 (1999).
47. Huot, S., Buylaert, J.-P. & Murray, A. S. Isothermal thermoluminescence signals from quartz. *Radiat. Meas.* **41**, 796–802 (2006).
48. Thomsen, K. J., Murray, A. S., Jain, M. & Botter-Jensen, L. Laboratory fading rates of various luminescence signals from feldspar-rich sediment extracts. *Radiat. Meas.* **43**, 1474–1486 (2008).
49. Hütt, G., Jaek, I. & Tchonka, J. Optical dating: K-feldspars optical response stimulation spectra. *Quat. Sci. Rev.* **7**, 381–385 (1988).
50. Buylaert, J. P., Murray, A. S., Thomsen, K. J. & Jain, M. Testing the potential of an elevated temperature IRSL signal from K-feldspar. *Radiat. Meas.* **44**, 560–565 (2009).
51. Murray, A. S., Buylaert, J. P., Thomsen, K. J. & Jain, M. The effect of preheating on the IRSL signal from feldspar. *Radiat. Meas.* **44**, 554–559 (2009).
52. Thiel, C. et al. Luminescence dating of the Stratzing loess profile (Austria)—testing the potential of an elevated temperature post-IR IRSL protocol. *Quat. Int.* **234**, 23–31 (2011).
53. Thomsen, K. J., Murray, A. S. & Jain, M. Stability of IRSL signals from sedimentary K-feldspar samples. *Geochronometria* **38**, 1–13 (2011).
54. Stokes, S. et al. Alternative chronologies for late Quaternary (last interglacial–Holocene) deep sea sediments via optical dating of silt-sized quartz. *Quat. Sci. Rev.* **22**, 925–941 (2003).
55. Mejdahl, V. Thermoluminescence dating: beta-dose attenuation in quartz grains. *Archaeometry* **21**, 61–72 (1979).
56. Feathers, J. K. & Migliorini, E. Luminescence dating at Katanda—a reassessment. *Quat. Sci. Rev.* **20**, 961–966 (2001).
57. Huntley, D. J. & Baril, M. R. The K content of the K-feldspars being measured in optical dating or in thermoluminescence dating. *Ancient TL* **15**, 11–13 (1997).
58. Huntley, D. J. & Hancock, R. G. V. The Rb contents of the K-feldspars being measured in optical dating. *Ancient TL* **19**, 43–46 (2001).
59. Prescott, J. R. & Hutton, J. T. Cosmic-ray contributions to dose rates for luminescence and ESR dating: large depths and long-term time variations. *Radiat. Meas.* **23**, 497–500 (1994).
60. Rivera, T. A., Storey, M., Schmitz, M. D. & Crowley, J. L. Age intercalibration of $^{40}Ar/^{39}Ar$ sanidine and chemically distinct U/Pb zircon populations from the Alder Creek Rhyolite Quaternary geochronology standard. *Chem. Geol.* **345**, 87–98 (2013).
61. Brumm, A. et al. Hominins on Flores, Indonesia, by one million years ago. *Nature* **464**, 748–752 (2010).
62. Storey, M., Roberts, R. G. & Saidin, M. Astronomically calibrated $^{40}Ar/^{39}Ar$ age for the Toba supereruption and global synchronization of late Quaternary records. *Proc. Natl Acad. Sci. USA* **109**, 18684–18688 (2012).
63. Eggins, S., Grün, R., Pike, A. W. G., Shelley, A. & Taylor, L. ^{238}U, ^{232}Th profiling and U-series isotope analysis of fossil teeth by laser ablation-ICPMS. *Quat. Sci. Rev.* **22**, 1373–1382 (2003).
64. Grün, R. et al. U-series and ESR analyses of bones and teeth relating to the human burials from Skhul. *J. Hum. Evol.* **49**, 316–334 (2005).
65. Grün, R. et al. ESR and U-series analyses of enamel and dentine fragments of the Banyoles mandible. *J. Hum. Evol.* **50**, 347–358 (2006).
66. Grün, R., Aubert, M., Joannes-Boyau, R. & Moncel, M. H. High resolution analysis of uranium and thorium concentrations as well as U-series isotope distributions in a Neanderthal tooth from Payre using laser ablation ICP-MS. *Geochim. Cosmochim. Acta* **72**, 5278–5290 (2008).
67. Grün, R. et al. ESR and U-series analyses of teeth from the palaeoanthropological site of Hexian, Anhui Province, China. *J. Hum. Evol.* **34**, 555–564 (1998).
68. Grün, R., Eggins, S., Kinsley, L., Moseley, H. & Sambridge, M. Laser ablation U-series analysis of fossil bones and teeth. *Palaeogeogr. Palaeoclimatol. Palaeoecol.* **416**, 150–167 (2014).
69. Joannes-Boyau, R. & Grün, R. A comprehensive model for CO_2^- radicals in fossil tooth enamel: implications for ESR dating. *Quat. Geochronol.* **6**, 82–97 (2011).
70. Joannes-Boyau, R. Detailed protocol for an accurate non-destructive direct dating of tooth enamel fragment using electron spin resonance. *Geochronometria* **40**, 322–333 (2013).
71. Joannes-Boyau, R., Duval, M. & Bodin, T. MCDoseE 2.0 A new Markov chain Monte Carlo program for ESR dose response curve fitting and dose evaluation. *Quat. Geochronol.* **44**, 13–22 (2018).
72. Shao, Q., Bahain, J. J., Dolo, J. M. & Falguères, C. Monte Carlo approach to calculate US-ESR age and age uncertainty for tooth enamel. *Quat. Geochronol.* **22**, 99–106 (2014).
73. Guérin, G., Mercier, N. & Adamiec, G. Dose rate conversion factors: update. *Ancient TL* **29**, 5–8 (2011).
74. Bronk Ramsey, C. Radiocarbon calibration and analysis of stratigraphy: the OxCal program. *Radiocarbon* **37**, 425–430 (1995).

Acknowledgements This research, including the Solo River survey and the Sembungan and Menden terrace excavations, was funded by the Australian Research Council Discovery grant (DP1093049) to K.E.W. and (DP0343334 and DP0770234) to M.J.M. The 2008–2010 excavations at Ngandong were supported by the Wenner-Gren Foundation for Anthropological Research (ICRG-92), University of Iowa (UI) Center for Global and Regional Environmental Research (CGRER), UI Office of the President, UI Dean of the College of Liberal Arts and Sciences and the UI Office of the Vice-President for Research (to R.L.C.). The Menden excavations were financially supported by the Geological Survey Institute in Bandung (GSI). Laboratory costs were funded, in part, by the Human Evolution Research Fund at the University of Iowa Foundation. The $^{40}Ar/^{39}Ar$ dating was funded by the Villum Foundation. The authors acknowledge the invaluable support provided by A. D. Wirakusaman, and the support of E. A. Subroto. Excavations at Sembungan were undertaken under a recommendation letter from the Provincial Government of West Java to the Governor of the Central Java Province no. 070.10/237; a recommendation letter from the latter to the local government of the Blora Regency no. 070.10/237; and a research permit issued by the Blora Regency no. 071/457/2005. Excavations at Ngandong were carried out with the permission and recommendation of Wahyu, Head of the Foreign Researchers Licensing Secretariat of the State Ministry of Research and Technology (SMRT), which issued research permits 03799/SU/KS/2006, 1718/FRP/SM/VII/2008, and 04/TKPIPA/FRP/SM/IV/2010 for the fieldwork at Ngandong. The excavations at Sembungan and the Menden Terrace site in the Blora Regency were carried out under research permit no. 2785/FRP/SM/XI/2008. We thank K. M. Patel for help with figure creation and editorial assistance with the manuscript.

Author contributions Y.R., Y.Z., E.A.B. III, O.F.H., R.L.C., R.G., A., M.E.S., R.L., R.S. and S.P. carried out the 2008 and 2010 excavations at Ngandong, organized by Y.Z. and R.L.C. The Solo River survey and Sembungan and Menden terrace excavations were carried out by K.E.W., M.J.M., G.D.v.d.B., Sidarto, I.K., M.W.M., F.A. and Suminto. Dating of samples and age modelling was conducted by K.E.W., R.G., R.J.-B., R.M.B., M.S., J.-x.Z. and faunal analysis by R.S., J.-P.Z. and G.D.v.d.B. M.W.M. analysed the stone artefacts from Sembungan. This manuscript was written and edited by K.E.W., R.L.C., M.C.W., O.F.H., G.D.v.d.B., E.A.B. III and R.L. with sections of the Methods and Supplementary Information written by K.E.W., O.F.H., R.L.C., E.A.B. III, R.G., R.M.B., J.-x.Z., M.W.M. and M.S. All authors commented on and contributed to the manuscript.

Competing interests The authors declare no competing interests.

Additional information

Supplementary information is available for this paper at https://doi.org/10.1038/s41586-019-1863-2.

Correspondence and requests for materials should be addressed to K.E.W. or R.L.C.

Peer review information *Nature* thanks Robin Dennell, James K. Feathers, Edward J. Rhodes and the other, anonymous, reviewer(s) for their contribution to the peer review of this work.

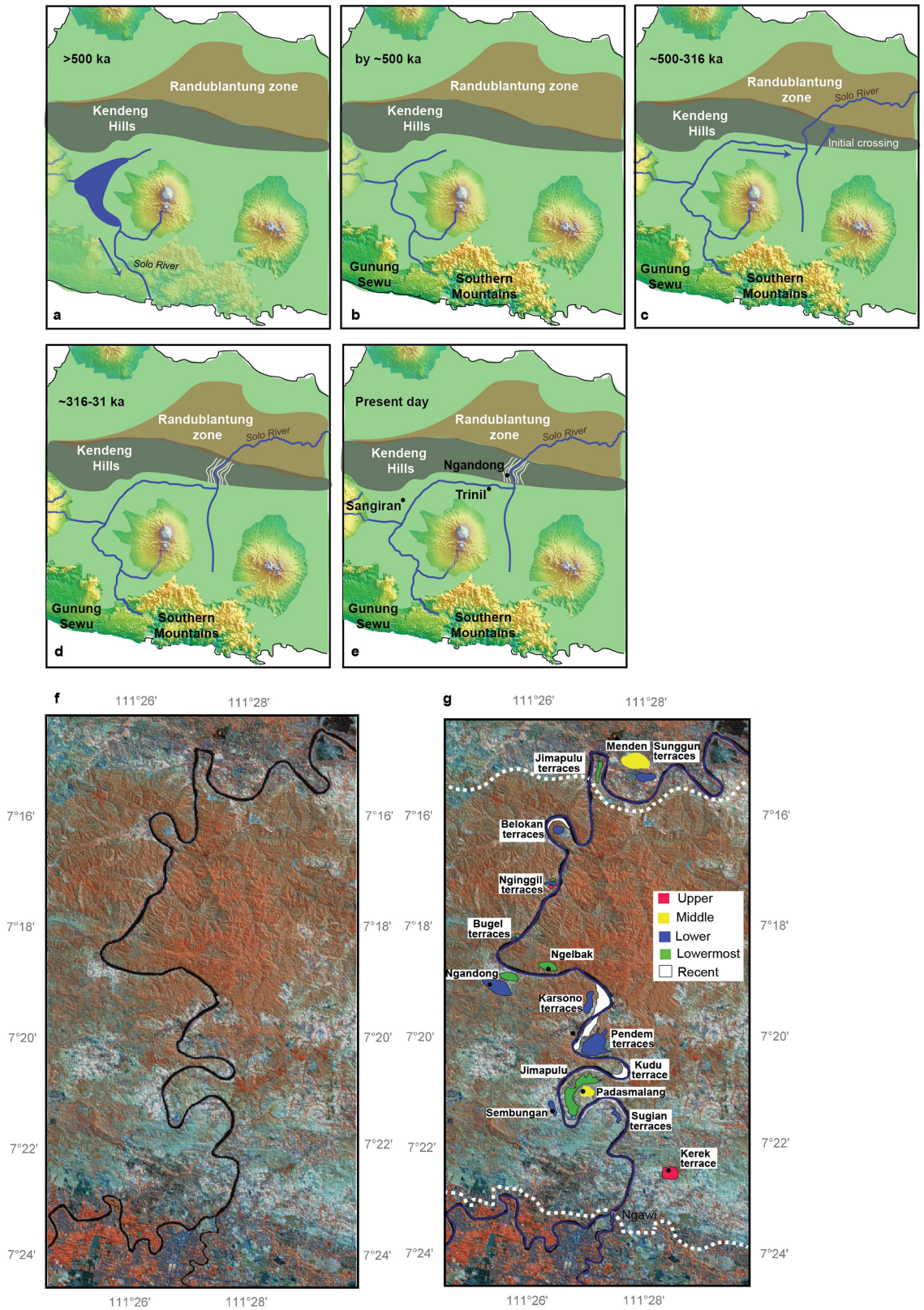

Extended Data Fig. 1 | See next page for caption.

Extended Data Fig. 1 | Evolutionary and geomorphical history of region. The landscape evolutionary stages that created the Solo River terraces. Drawn from refs. [2,3] on a topographical map from the USGS EROS. **a**, More-than 500-ka drainage from the proto-Merapi and Lawu volcanic highlands formed a lake or lagoon from which the proto-Solo River drained to the south (blue arrow), close to the present-day Pacitan region, and another branch flowed to the north of Lawu. By at least 1.5 million years ago, the Southern Mountains to the south and the Kendeng anticlinorium to the north were slowly emerging, forming the Gunung Sewu, and the Kendeng Hills (previously the Randublantung marine embayment[2]), respectively. **b**, By about 500 ka, the seismically uplifted Southern Mountains had blocked the southern exit of the Solo River to the ocean, and the area was dominated by trunk streams of the Solo River. **c**, Between about 500 and 316 ka, the Solo River abandons its southern trunk stream and extends its northern branch, where it is diverted to the west and northeast and carves an initial crossing through the Kendeng Hills to form the Solo River gap, and drain into the ocean to the north of Surabaya. **d**, Between about 316 and 31 ka, the uplifting Kendeng anticlinorium and the drainage from the Madiun Basin energized the Solo River, causing incision and forming the Solo River sequence of terraces (white parallel lines). **e**, Present-day Solo Basin and known fossil sites on exposed terraces. **f**, A digital elevation model[31,32], comprising a satellite image overlying a topographical map of the section of the Solo River system from Kerek village in the south to Sunggun village in the north (USGS Landsat). **g**, The same digital elevation model, with the classification scheme for the Solo River terraces with the upper, middle, lower and lowermost terraces identified. This image includes the key terrace sites that are sampled in this study; Kerek (upper), Padasmalang (middle), Sembungan (lower), Nglebak (lowermost) and Menden (outside of the Kendeng Hills, but contemporaneous with the upper and middle terraces), and the key fossil site of Ngandong (lower). The white dashed line indicates the limits of the Kendeng Hills. The Menden terrace lies outside of this divide, as does the westward-bearing Solo River and the site of Trinil.

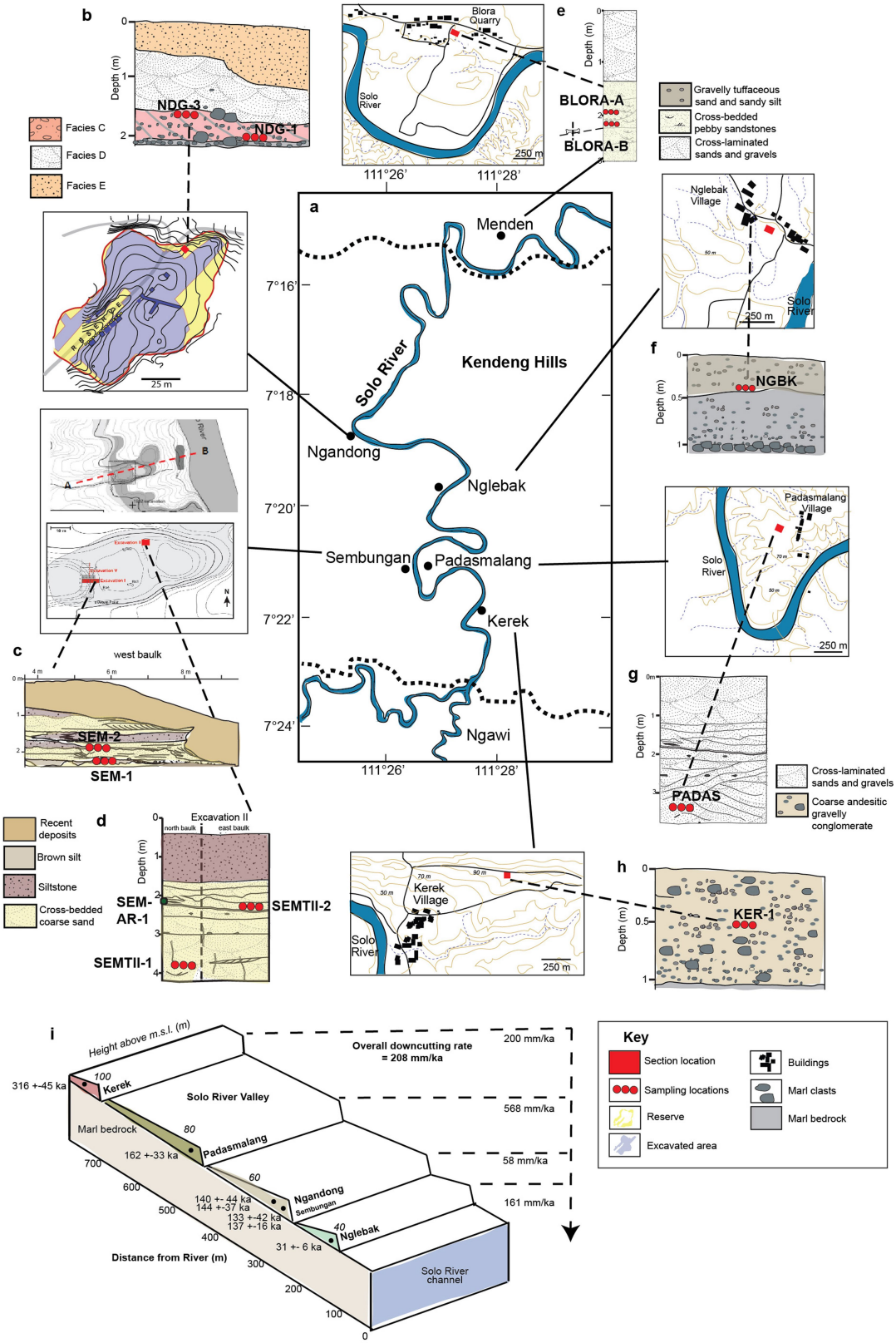

Extended Data Fig. 2 | Terrace-site stratigraphy and luminescence sampling. **a**, Map of the Kendeng Hills section of the Solo River from Ngawi to Menden, displaying the location of the six studied sites. Each site has a smaller inset showing the site locations, stratigraphic sections of the strath terraces and sampling locations for luminescence dating. **b**, Ngandong; the inset for the Ngandong site is shown in more detail to identify the exact location of the sampling site within the context of previous excavations. **c**, Sembungan excavation I. **d**, Sembungan excavation II. **e**, Menden. **f**, Nglebak. **g**, Padasmalang. **h**, Kerek. **i**, Three-dimensional slice of the Solo River valley, showing the terrace sequences and resulting downcutting rates (derived from 21 terrace samples ($n = 21$), mean ages with uncertainties presented at 1σ) plotted according to elevation and distance away from the river. The associated downcutting rates have been presented for each terrace, and for the river system as a whole.

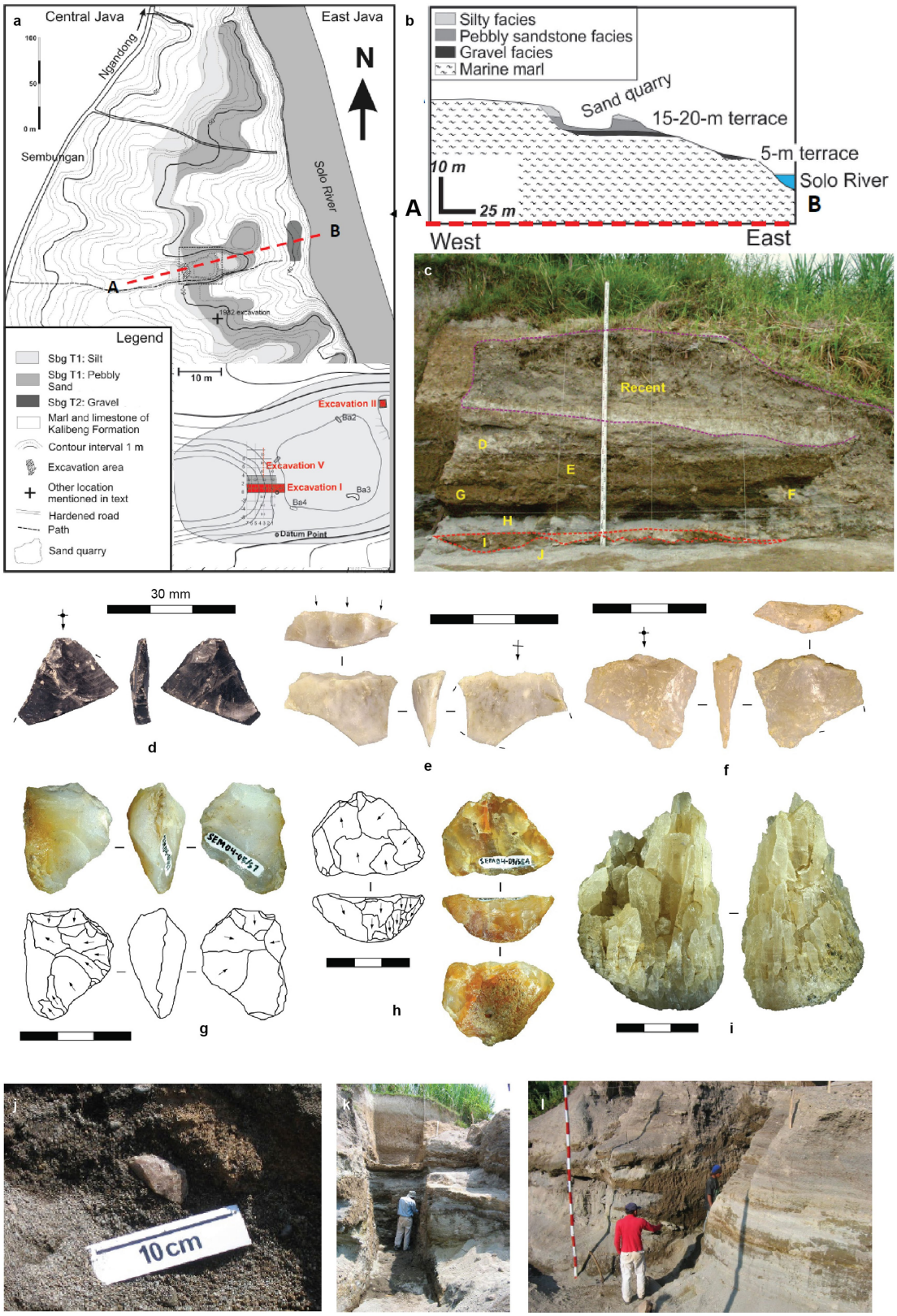

Extended Data Fig. 3 | See next page for caption.

Extended Data Fig. 3 | Stratigraphy and artefacts of the Sembungan excavations. a, Map of the Sembungan terrace, showing the lithology of the terrace and the location of the terrace rise in relation to the Solo River. The bottom-right inset shows the locations of the excavations I, II and V. **b**, A profile of the terrace along the A–B transect from A (marked by a red dashed line), showing the location of the sand quarry excavations in relation to the river. **c**, The west baulk of excavation I (marked on the inset in A), showing the stratigraphic layers and location of the stone artefact concentration (red dashed line at the base of the section). Layer J, very coarse sand; layer I, brown silt; layer H, cross-bedded coarse pebbly sand; layer G, lenses of siltstone; layer F, disturbed; layer E, massive siltstone; layer D, caliche palaeosol. **d**–**i**, Stone artefacts excavated in situ from Sembungan. **d**, Obsidian flake. **e**, Chert flake with unifacial retouching to the ventral surface across the proximal end, removing the point of force application. **f**, Chalcedony flake. **g**, **h**, Chalcedony centripetal cores. **i**, Quartz crystal cluster. Scale bars, 30 mm. **j**, A stone tool in situ from the Sembungan excavation V. **k**, Excavation I (inset in **a**). **l**, Excavation II (inset in **a**).

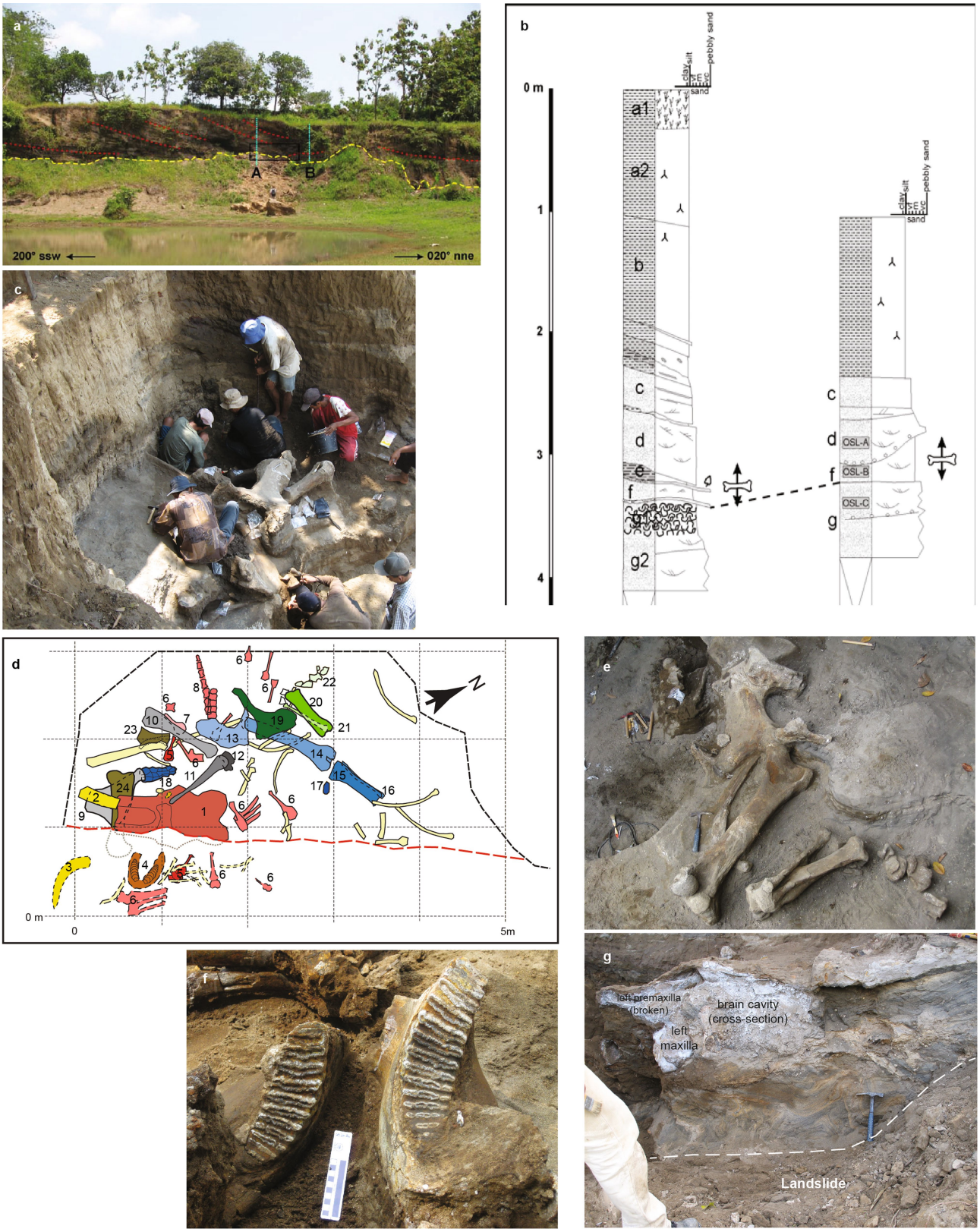

Extended Data Fig. 4 | See next page for caption.

Extended Data Fig. 4 | Menden stratigraphy and fossils. a, The quarry site of Blora on the Menden terrace near Sunggu (Central Java, Indonesia), to the north of the Kendeng Hills. The red dashed lines depict mega cross-bedding in the fluvial terrace. The vertical blue lines correspond to the stratigraphic section shown in **b** the yellow dashed line depicts the landslide scarp, and the black box shows the location of an almost-complete elephant skeleton. **b**, The stratigraphy of the Menden terrace according to logs A and B (marked on **a**). The upper a1, a2 and b layers represent cross-laminated sands and gravels, and the lower c–g layers represent cross-bedded pebbly sandstones. The relative location of the elephant skeleton can be seen by the fossil symbol. **c**, The excavation of the Menden terrace to recover the elephant skeleton (*Elephas hysudrindicus*)—a rare elephant species, endemic to Java. **d**, Site plan of the partial *E. hysudrindicus* skeleton excavated from the Menden terrace. Thick dashed line indicates extension of the excavation. Red dashed line indicates the boundary of the quarry wall at the time the fossil was discovered. All fossils recovered south of this boundary were found in a landslide at the foot of the quarry wall. 1, partial skull; 2, right tusk; 3, left tusk; 4, mandible; 5, cervical vertebrae; 6, thoracic vertebrae; 7, lumbar vertebrae; 8, caudal vertebrae; 9, right scapula; 10, right humerus; 11, right radius; 12, right carpals; 13, right pelvis; 14, right femur; 15, right tibia; 16, right fibula; 17, right patella; 18, right pes (articulated); 19, left pelvis; 20, left tibia; 21, left radius; 22, left tarsals; 23, left scapula fragment; 24, left humerus; pale yellow bones are ribs. **e**, The right pelvis and femur of the elephant in articulation, lying next to the left tibia and fibula and tarsals. **f**, The broken lower jaw of the elephant, with teeth, recovered from the landslide. **g**, The skull of the elephant in cross-section, as found in the landslide scar. Convoluted sediment layers can be seen below the skull.

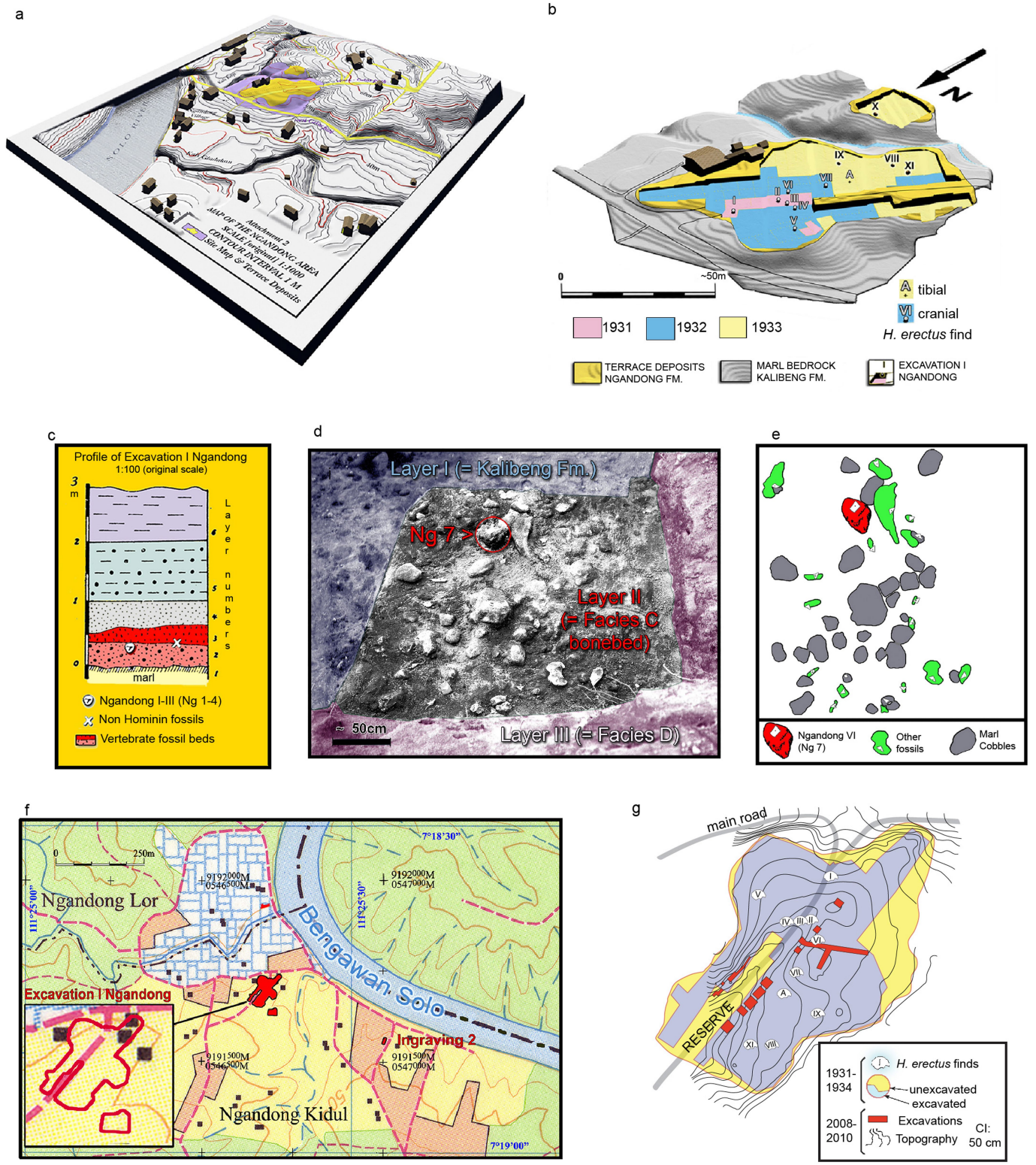

Extended Data Fig. 5 | History of *H. erectus* excavations at Ngandong. **a**, Aerial view of Ngandong, created from an unpublished map produced by the Geological Survey of the Netherlands Indies, who discovered the site and documented the unearthing of 14 *H. erectus* specimens. **b**, Extent of the 27-month-long, 1931–1933 excavations, including *H. erectus* finds[3]. The excavations produced about 25,000 fossils from the Ngandong terrace (originally referred to as the 20-m terrace) deposits[3]. **c**, Redisplay and translation of an original stratigraphic profile, published by the Geological Survey of the Netherlands Indies, showing the first four *H. erectus* discoveries made in 1931[3,4]. **d**, Day-of-discovery photograph of Ngandong VI (Ng 7), which is a whole fossil calvaria[3]. **e**, Plan-view drawing of the excavation square that included Ngandong VI, embedded in a river deposit of very coarse-grained volcaniclastic sand, along with marl cobbles and other vertebrate fossils[3]. **f**, Location of the site in the greater Ngandong area. **g**, Total data station mapping allowed the 1931–1933 excavated area to be repositioned on the landscape, including the 1931–1933 *H. erectus* discovery points (Extended Data Fig. 6). Panels **a**–**f** are redrawn from a previous publication[3].

Extended Data Fig. 6 | Photographs of 2008 and 2010 excavations at Ngandong including fossil discoveries. a, View of Ngandong site before the 2008 excavation, facing northwest. The orange string line marks the extent of the 1931–1933 excavations[3]. **b**, Collection of samples for optically stimulated luminescence dating, from facies B and C in pit A from 2008 (excavation unit H10a of the 2010 excavation). **c**, Bovid scapula and other fossils found in facies C in H10a from 2010. **d**, Excavations underway in excavation units H10a (foreground) and H10c (being dug) in 2010. **e**, Stratigraphy seen in the northwest wall of excavation unit H10a in 2010. Facies E is seen above the remnant of facies A, B, C and D, which are visible in the bottom half of this section. **f**, Exposed bone bed in facies A and C in excavation unit G09 from 2010. **g**, Fossils collected during 2010 excavation. Photographs **a**, **c** and **e** are by O.F.H. All other photographs are by R.L.C.

Extended Data Fig. 7 | Fauna from Ngandong recovered during the 2008–2010 excavations. a, Cervid antler, cf. *Axis* sp., specimen NDG 2306. **b**, Lower right M3, cf. *Bos* sp., specimen NDG 1134. **c**, Bovid incisor (Ix), cf. *Bubalus* sp. NDG 1106. **d**, Bovid cervical vertebra (atlas), specimen NDG 2149. **e**, Bovid tooth (*Bubalus* sp.), specimen NDG 1131. **f**, Cervid tooth, cf. *Cervus* sp., specimen NDG 2074. **g**, Bovid tooth (*Bubalus* sp.), specimen NDG 1038. **h**, Bovid tooth (*Bubalus* sp.), specimen NDG 2569. **i**, Bovid tooth (*Bubalus* sp.), specimen NDG 1163. **j**, Artiodactyl canon bone, specimen NDG 2148. **k**, Artiodactyl hoof, specimen NDG 2199. Specimens NDG-1038, NDG-1163 and NDG-2569 (**e**, **g** and **i**) provided results for US–ESR age calculations (Extended Data Fig. 10). All photographs are by J.-P.Z.

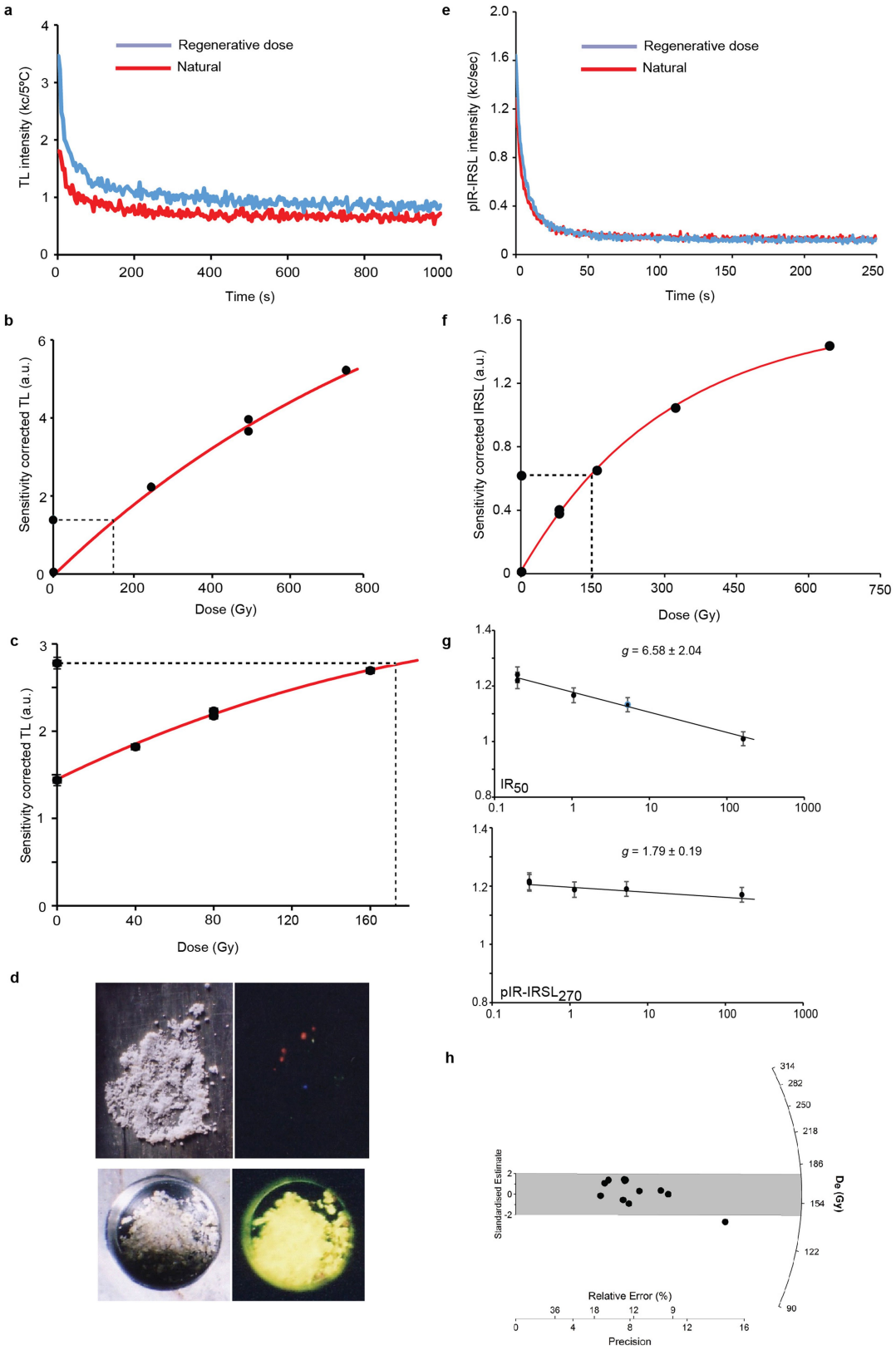

Extended Data Fig. 8 | See next page for caption.

Extended Data Fig. 8 | A comparison of red thermoluminescence and pIR-IRSL luminescence data for sample NDG-1. a, Quartz red thermoluminescence isothermal decays, showing a natural and regenerative decay. **b**, The dose response of aliquot A of the DAP technique with a D_e value of 185 ± 53 Gy. The points represent the mean with s.d. uncertainties (too small to see at this scale). **c**, The dose response of the subtracted aliquot B of the DAP technique with a D_e value of 170 ± 53 Gy. The points represent the mean value with an error as a s.d. of the fit (too small to see at this scale). **d**, Photographs of the luminescence emitted by a sample from the Ngandong terrace (NDG-1) compared to a sample from the Wae Raceng terrace in Flores (WR-1). The Flores terrace is so bright it has bleached the photographic paper, whereas the Ngandong terrace is much dimmer but the red luminescence emissions are clearly visible. **e**, Feldspar pIR-IRSL decays for sample NDG-1, showing the natural and regenerative decays. A long stimulation time is required to remove all of the pIR-IRSL signal. **f**, A dose–response curve for the sample NDG-1 with a D_e value of 150 ± 4 Gy. Each dose point represents the mean value with s.d. uncertainties (too small to see at this scale). **g**, Fading tests for the sample NDG-1, comparing the fading of the infrared signal at 50 °C (IR_{50}) with the fading with the pIR-IRSL signal at 270 °C ($pIR\text{-}IRSL_{270}$)—demonstrating the isolation of a very small fading signal. The points represent the median value with a standard error. **h**, Radial plot of the NDG-1 single-aliquot data.

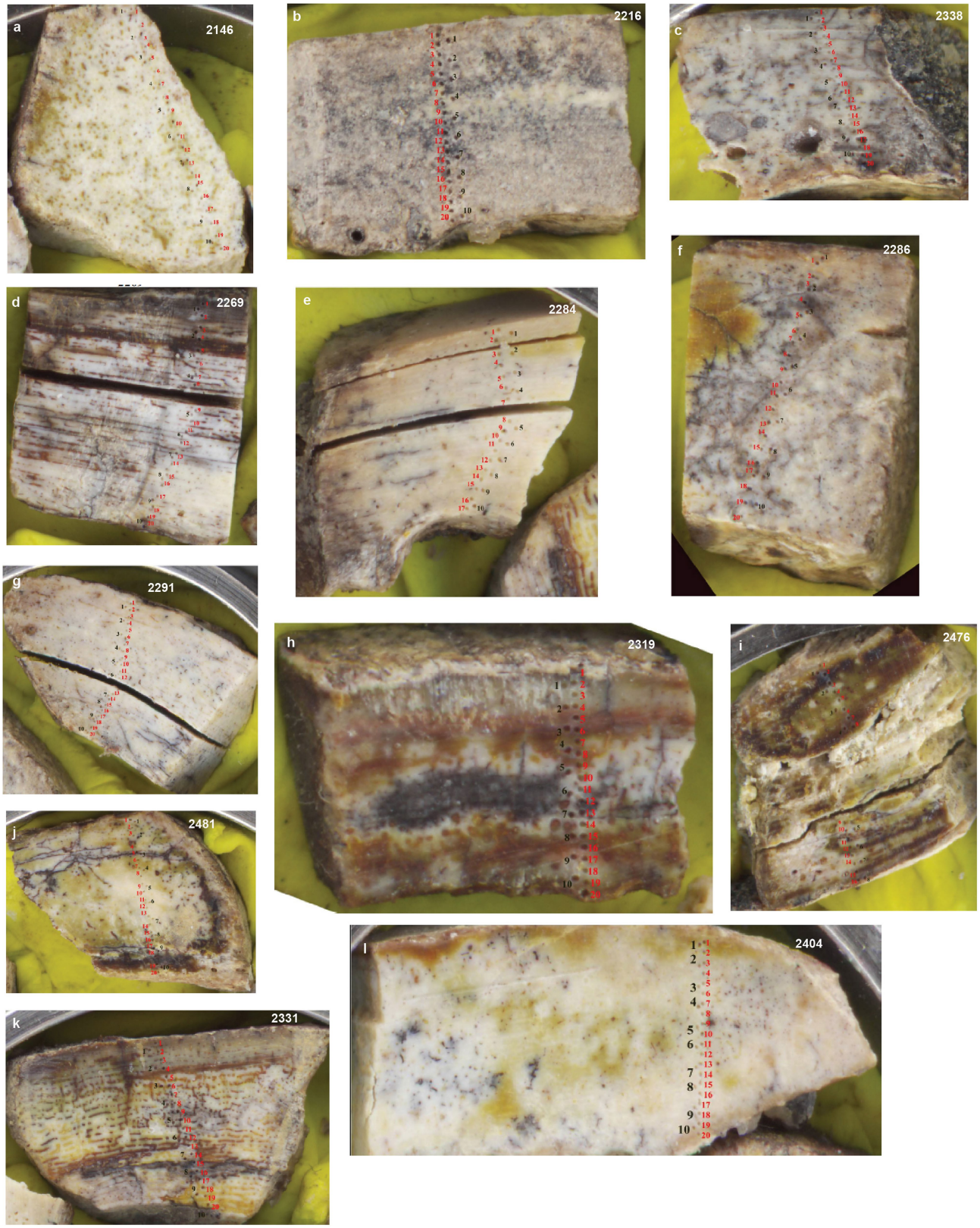

Extended Data Fig. 9 | U-series-age depth dating of bone. a–l, Fossil bone recovered from the Ngandong excavations in 2010, displaying the track lines created by the LA-ICP-MS for U-series-age depth modelling. Bones were recovered from facies A and C. Figure 2 gives the locations of the bones. Specimen numbers (NDG) for each bone are listed in white in the top right corner.

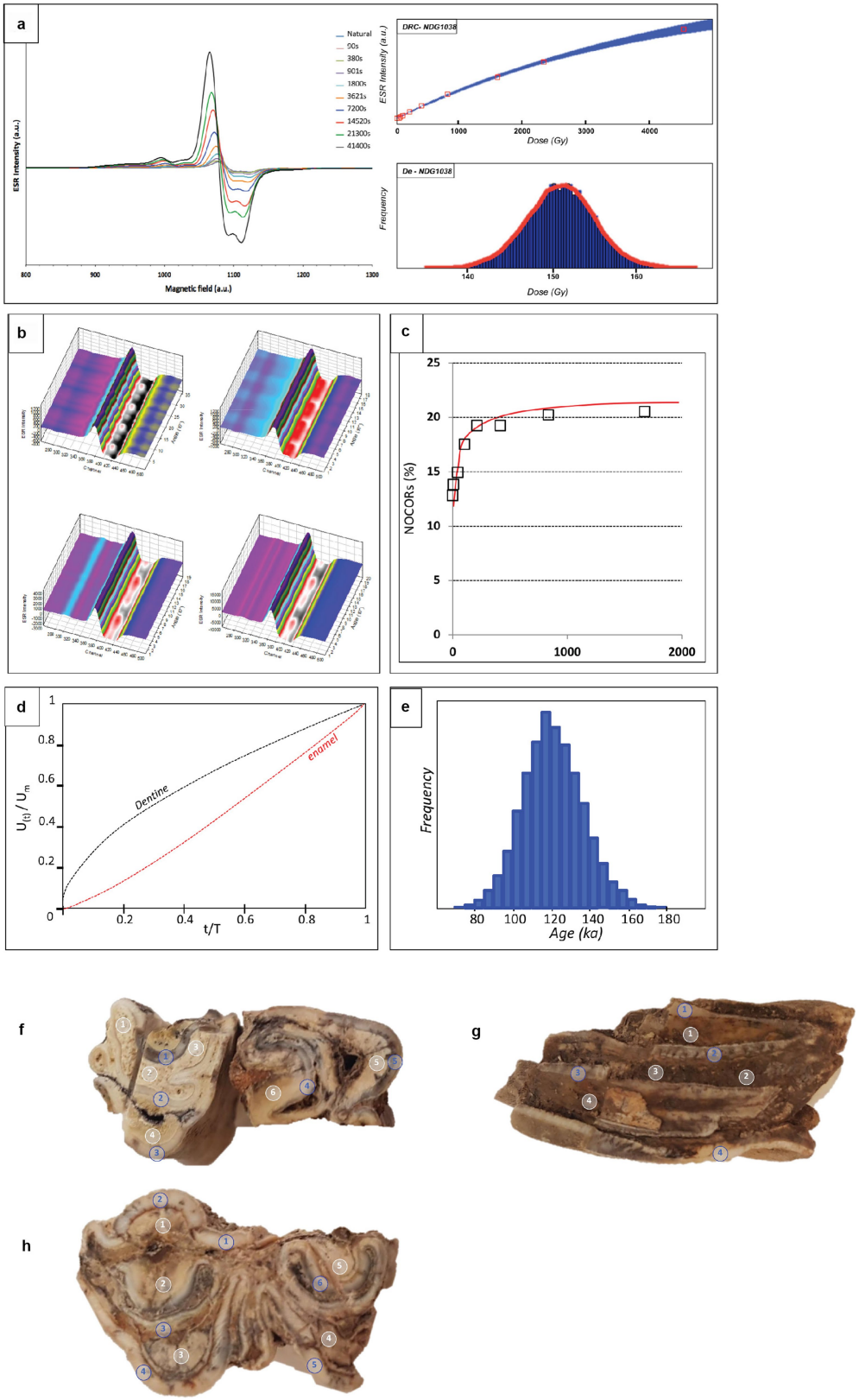

Extended Data Fig. 10 | See next page for caption.

Extended Data Fig. 10 | Summary of the US–ESR dating protocol, and results for sample NDG-1038. a, Left, spectra of the merged signal increasing with irradiation steps. Top right, double saturated exponential dose–response curve of NDG-1038, using the MCDoseE 2.0 program[71]. Bottom right, dose equivalent distribution, using the MCDoseE 2.0 program[71]. **b**, Angular response of the enamel fragment in the ESR spectrometer at various irradiation steps from left to right and top to bottom: natural, 380 s, 1,800 s and 7,200 s. **c**, Determination of the NOCOR percentage in the angular response after subtracting the natural signal[70]. **d**, Uranium-uptake model in both enamel (red) and dentine (black) used to calculate the US–ESR dating of NDG-1038. **e**, US–ESR age distribution for NDG-1038 using a previously published program[72]. **f**–**h**, Photographs of the three bovid molar teeth. **f**, NDG-1038. **g**, NDG-11163. **h**, NDG-2569. These teeth were used for the direct dating by US–ESR of the Ngandong bone bed, with indication of U-series measurement locations. Teeth were sectioned to expose the various dental tissues. Numbers in white circles correspond to the dentine, and numbers in blue circles correspond to the enamel measurements. Results for each laser spot can be found in the Supplementary Table 8.

nature research

Corresponding author(s): Ciochon

Last updated by author(s): Oct 7, 2019

Reporting Summary

Nature Research wishes to improve the reproducibility of the work that we publish. This form provides structure for consistency and transparency in reporting. For further information on Nature Research policies, see Authors & Referees and the Editorial Policy Checklist.

Statistics

For all statistical analyses, confirm that the following items are present in the figure legend, table legend, main text, or Methods section.

n/a	Confirmed	
☐	☒	The exact sample size (*n*) for each experimental group/condition, given as a discrete number and unit of measurement
☐	☒	A statement on whether measurements were taken from distinct samples or whether the same sample was measured repeatedly
☐	☒	The statistical test(s) used AND whether they are one- or two-sided *Only common tests should be described solely by name; describe more complex techniques in the Methods section.*
☒	☐	A description of all covariates tested
☐	☒	A description of any assumptions or corrections, such as tests of normality and adjustment for multiple comparisons
☐	☒	A full description of the statistical parameters including central tendency (e.g. means) or other basic estimates (e.g. regression coefficient) AND variation (e.g. standard deviation) or associated estimates of uncertainty (e.g. confidence intervals)
☒	☐	For null hypothesis testing, the test statistic (e.g. *F*, *t*, *r*) with confidence intervals, effect sizes, degrees of freedom and *P* value noted *Give P values as exact values whenever suitable.*
☐	☒	For Bayesian analysis, information on the choice of priors and Markov chain Monte Carlo settings
☒	☐	For hierarchical and complex designs, identification of the appropriate level for tests and full reporting of outcomes
☒	☐	Estimates of effect sizes (e.g. Cohen's *d*, Pearson's *r*), indicating how they were calculated

Our web collection on statistics for biologists contains articles on many of the points above.

Software and code

Policy information about availability of computer code

Data collection	All software used for data collection is commercially available or described in the published literature (citations included). Software used includes: Microsoft Excel and MCDoseE (version 2.0) (for ESR dating).
Data analysis	All software used for data collection is commercially available or described in the published literature. Software used includes: Microsoft Excel, Isoplot EX (version 3.75) (U-series), MATHLAB USESR (US-ESR), OxCal (version 4.2) (Bayesian modeling), Riso Sequence Pro and Analyst. Full OxCal code for the Bayesian modeling is provided in Supplementary Table 15.

For manuscripts utilizing custom algorithms or software that are central to the research but not yet described in published literature, software must be made available to editors/reviewers. We strongly encourage code deposition in a community repository (e.g. GitHub). See the Nature Research guidelines for submitting code & software for further information.

Data

Policy information about availability of data

All manuscripts must include a data availability statement. This statement should provide the following information, where applicable:

- Accession codes, unique identifiers, or web links for publicly available datasets
- A list of figures that have associated raw data
- A description of any restrictions on data availability

The data that support the findings of this study are included in the Supplementary Information. Additional data is available from the corresponding author upon reasonable request.

Field-specific reporting

Please select the one below that is the best fit for your research. If you are not sure, read the appropriate sections before making your selection.

☐ Life sciences ☐ Behavioural & social sciences ☒ Ecological, evolutionary & environmental sciences

For a reference copy of the document with all sections, see nature.com/documents/nr-reporting-summary-flat.pdf

Ecological, evolutionary & environmental sciences study design

All studies must disclose on these points even when the disclosure is negative.

Study description	To determine the age of the hominin site of Ngandong, we considered three interrelated components; a landscape context, a terrace context, and a fossil context. Samples were dated using Uranium-series dating of speleothems, red TL, pIR-IRSL, 40Ar/39Ar, U-series on fossils, and ESR on fossil teeth. In total, we provide a modelled site age using 52 radiometric ages estimates. The study also includes the analysis of fossils and artefacts recovered from the contemporary sites of Ngandong, Sembungan, and Menden.
Research sample	To constrain the site of Ngandong we choose samples from a landscape, regional and local perspective. We chose speleothem samples from the 5 highest individual cave systems in the Gunung Sewu region. We chose optimum terrace sites from a large terrace survey conducted by the GRDC. Finally we determined excavation locations at Ngandong from extensive analysis of previous excavation to determine the original in situ locations and conducted multiple excavation baulks in these locations to optimise the sampling potential.
Sampling strategy	To establish a statistically significant sample size our sampling strategy was to sample from multiple locations in the Ngandong region as described above. Five speleothem samples were collected from the highest (therefore the oldest) caves sites in the Gunung Sewu – this number allows the oldest age range of speleothem precipitation to be estimated. We collected 21 luminescence and Ar-Ar samples from six different terraces in six different locations in the Ngandong area. By sampling this widely, we were able to robustly constrain each of the steps of terrace evolution in the Solo Valley. The chronology of the terraces were tested with independent age estimates from three different luminesce dating techniques (Red TL heat reset, Red TL light reset and pIR-IRSL techniques) and Ar-Ar dating. To constrain the fossil assemblage in the Ngandong terrace were conducted 26 direct dating age estimates of the bone and teeth from throughout the terrace across all four of the named Facies (A-D). Samples were chosen according to the weathering state of the enamel/dentine or collagen. Particular emphasis was placed on dense, thick bones without cortical sections. Such bones come closest to conform to the general assumption of the diffusion adsorption model. By developing a comprehensive sedimentological and fossil context, our dating strategy produces a robust chronology for the Ngandong evidence. In regards to the sampling strategy for the excavation at Ngandong, we excavated pits on both sides of the 1930's archaeological reserve (5 pit in 2008 and 12 pits in 2010) across the Ngandong terrace and collected 867 specimens. In respect to the specimens collected by previous excavations, our sample is limited to the published literature and a small collection of fossils because the majority of the 1930's collection was lost during World War II.
Data collection	The Ngandong excavation data was recorded by the members of ITB including palaeontologists and archaeologists over two field periods (2008 and 2010). The Solo Terrace data was collected by GSI over a five year period. All data pertaining to the dating techniques were collected by the appropriate dating specialists during collection in 2008 and during laboratory analysis from 2008-2019.
Timing and spatial scale	Excavations and field data collection were conducted between 2005 and 2010 at multiple sites in the Solo River Valley, Central Java, Indonesia.
Data exclusions	Samples were excluded if they failed predetermined tests for each dating method. These tests and exclusion criteria are outlined for each dating method in the Methods Summary and Supplementary Information. Fragmentary fossils that could not be identified were excluded from analysis for the excavations. For the US-ESR dating of three teeth samples NDG-2074, NDG-2562 and NDG-2566 were excluded from the dating as no enamel layer offered a uranium concentration <5 ppm, which has been described as the maximum acceptable concentration within the enamel layer to obtain a reliable equivalent dose. The ESR dating of the 15 bone samples did not yield any meaningful results as porous bones often display considerably more complex U-migration paths. For the luminescence dating single-aliquots were rejected according to a rejection criteria devised by cited reference.
Reproducibility	Multiple samples (52) and dating methods (seven) were used to determine a chronology for the Ngandong evidence. For both the sedimentological and fossil context independent ages estimates were employed to guarantee that the results are reliable and reproducible. Age estimates are consistent and stratigraphically correct between samples.
Randomization	Samples were collected for a specific dating method. Fossil specimens were allocated into taxonomical groups.
Blinding	Blinding was not relevant to the sample dating or the archaeological and paleontological research.

Did the study involve field work? ☒ Yes ☐ No

Field work, collection and transport

Field conditions	Field sample collection and excavations took place at multiple location and times in the Solo River Valley, Central Java, Indonesia (tropical climate).

Location	Field sample collection and excavations took place at multiple sites in the Solo River Valley, Central Java, including Ngandong, Sembungan, Menden, Padasmalang, Kerek, and Nglebak as well Song Gupuh in Gunung Sewu, East Java (see Figure 1 for locations).
Access and import/export	Excavations at Sembungan were undertaken under a recommendation letter from the Provincial Government of West Java to the Governor of the Central Java Province No. 070.10/237; a recommendation letter from the latter to the local government of the Blora Regency No. 070.10/237; and a research permit issued by the Blora Regency No. 071/457/2005. Excavations at Ngandong were carried out with the permission and recommendation of Mr. Wahyu, Head of the Foreign Researchers Licensing Secretariat of the State Ministry of Research and Technology (SMRT) that issued research permits 03799/SU/KS/2006, 1718/FRP/SM/VII/2008, and 04/TKPIPA/FRP/SM/IV/2010 for the fieldwork at Ngandong. The excavations at Sembungan and the Menden Terrace site in the Blora Regency were carried out under Research Permit Number 2785/FRP/SM/XI/2008.
Disturbance	Excavation procedures and techniques followed national and local regulations.

Reporting for specific materials, systems and methods

We require information from authors about some types of materials, experimental systems and methods used in many studies. Here, indicate whether each material, system or method listed is relevant to your study. If you are not sure if a list item applies to your research, read the appropriate section before selecting a response.

Materials & experimental systems

n/a	Involved in the study
☒	☐ Antibodies
☒	☐ Eukaryotic cell lines
☐	☒ Palaeontology
☒	☐ Animals and other organisms
☒	☐ Human research participants
☒	☐ Clinical data

Methods

n/a	Involved in the study
☒	☐ ChIP-seq
☒	☐ Flow cytometry
☒	☐ MRI-based neuroimaging

Palaeontology

Specimen provenance	Fossils were recovered from excavations at Ngandong, Sembungan, and Menden. More details about the provenance of these fossils is included in the Supplementary Information. A full list of permits for the excavations can be found in the Acknowledgments and in "Access and import/export" above. Permits were obtained for all specimens that were removed from Java, Indonesia, for laboratory analysis.
Specimen deposition	Fossils recovered from the 2008-2010 excavations at Ngandong are housed at the Institut Teknologi Bandung, Indonesia. Fossils and arefacts from the Sembungan and Menden excavations are under the care of the GSI, Indonesia.
Dating methods	The Methods Summary and Supplementary Information provides detailed descriptions of each dating method. Uranium-series dating of the speleothem samples was conducted in the Radiogenic Isotope Facility of The University of Queensland using VG Sector 54 thermal ionisation mass spectrometer (TIMS) and a Nu Plasma multi-collector inductively coupled mass spectrometer (MC-ICP-MS). All luminescence analysis, red TL and pIR-IRSL, was conducted at the "Traps" luminescence dating facility at Macquarie University in Sydney, Australia using a TL-DA-20 Luminescence reader. Neutron irradiation for 40AR/39Ar dating of hornblende crystals was conducted in the cadmium-shielded CLICIT facility at the Oregon State University TRIGA reactor. Laser ablation mass spectrometry to measure U-series isotopes along the cross-sections of these dense, mammalian long-bone fossils were carried out at the Australian National University. U-series analysis of fossil teeth was conducted at the Australian National University. Additional U-series measurements and ESR measurements were undertaken at Southern Cross University.

☒ Tick this box to confirm that the raw and calibrated dates are available in the paper or in Supplementary Information.